bioRxiv preprint doi: https://doi.org/10.1101/2024.09.26.615271; this version posted September 27, 2024. The copyright holder for this preprint (which was not certified by peer review) is the author/funder, who has granted bioRxiv a license to display the preprint in perpetuity. It is made available under aCC-BY-NC-ND 4.0 International license.

Title:

Dysregulation of the fluid homeostasis system by aging

Authors:

Heeun Jang[1], Alexis B. Sharma[2], Usan Dan[2], Jasmine H. Wong[2], Zachary A. Knight[2,3,4]*, Jennifer L. Garrison[1,5,6,7]*

Affiliations:

[1] Buck Institute for Research on Aging, Novato, CA 94945, USA

[2] Department of Physiology;

[3] Kavli Institute for Fundamental Neuroscience;

[4] Howard Hughes Medical Institute;

University of California San Francisco, San Francisco, CA 94158, USA

[5] Center for Healthy Aging in Women, Novato, CA 94945, USA

[6] Cellular and Molecular Pharmacology, University of California, San Francisco, San Francisco, CA 94158, USA

[7] Leonard Davis School of Gerontology, University of Southern California; Los Angeles, CA 90089, USA.

*Co-corresponding authors

Lead Contact: jgarrison@buckinstitute.org

Keywords: thirst, fluid homeostasis, aging, SFO, PVH, AVP, hypothalamus, vasopressin, dehydration

bioRxiv preprint doi: https://doi.org/10.1101/2024.09.26.615271; this version posted September 27, 2024. The copyright holder for this preprint (which was not certified by peer review) is the author/funder, who has granted bioRxiv a license to display the preprint in perpetuity. It is made available under aCC-BY-NC-ND 4.0 International license.

SUMMARY

Chronic dehydration is a leading cause of morbidity for the elderly, but how aging alters the fluid homeostasis system is not well understood. Here, we used a combination of physiologic, behavioral and circuit analyses to characterize how fluid balance is affected by aging in mice. We found that old mice have a primary defect in sensing and producing the anti-diuretic hormone vasopressin, which results in chronic dehydration. Recordings and manipulations of the thirst circuitry revealed that old mice retain the ability to sense systemic cues of dehydration but are impaired in detecting presystemic, likely oropharyngeal, cues generated during eating and drinking, resulting in disorganized drinking behavior on short timescales. Surprisingly, old mice had increased drinking and motivation after 24-hour water deprivation, indicating that aging does not result in a general impairment in the thirst circuit. These findings reveal how a homeostatic system undergoes coordinated changes during aging.

BACKGROUND

Tight control of fluid balance is essential for life. This is achieved by a physiologic system that monitors the osmolality and volume of the blood and, in response to dehydration, triggers two counterregulatory responses: water consumption, which is motivated by the sensation of thirst, and water reabsorption by the kidney, which is triggered by the hormone vasopressin (AVP). These two responses are controlled by dedicated neural circuits in the forebrain that directly sense changes in fluid balance (reviewed in 1). Two key nodes in this forebrain circuitry are the subfornical organ (SFO), which contains glutamatergic neurons (SFO^{Glut} neurons) that are activated by increases in blood osmolality and decreases in blood volume to produce thirst (**Fig. 1a**), and AVP-expressing neurons in the supraoptic and paraventricular hypothalamic (PVH) nuclei , which produce and release AVP into the blood in response to upstream dehydration signals, including those arising from the SFO (**Fig. 1b**). These two nodes are interconnected with other forebrain nuclei that sense and process fluid balance information, including the organum vasculosum of the lamina terminalis (OVLT) and the median preoptic nucleus (MnPO; **Fig. 1a, b**).

Dysregulation of fluid homeostasis is a common feature of aging. For example, older adults report a reduced perception of thirst and consume less water after many thirst-evoking (dipsogenic) stimuli[2–9]. In addition, the ability of the kidney to concentrate urine declines with age, leading to greater loss of fluid

bioRxiv preprint doi: https://doi.org/10.1101/2024.09.26.615271; this version posted September 27, 2024. The copyright holder for this preprint (which was not certified by peer review) is the author/funder, who has granted bioRxiv a license to display the preprint in perpetuity. It is made available under aCC-BY-NC-ND 4.0 International license.

in older adults (reviewed in 10). As a result, aging is associated with increased prevalence of chronic dehydration[11], which is a significant risk factor for morbidity and mortality[12,13].

The specific alterations in the fluid homeostasis system that are caused by aging are not well understood. One challenge is that fluid balance involves multiple interacting systems, including a neuroendocrine system that controls water resorption (the AVP-kidney axis); a sensory system that monitors fluid balance and ingestion, which includes SFO^{Glut} neurons and their sensory afferents arising from the mouth, throat and viscera; and a motivational system which drives water seeking and consumption, which includes SFO^{Glut} neurons as well as their downstream targets such as the dopamine system. It has only recently become possible to monitor and manipulate these fluid homeostasis neurons in behaving animals[14–18], and no study has examined how any of these circuit nodes are altered by the aging process at the level of specific neural cell types, dynamics, and interconnections.

Here we have performed a comprehensive analysis of how the fluid homeostasis system is altered by aging in mice. We investigated animals of both sexes, across a range of ages from young to very old, and subjected them to batter of analyses at different levels, including: (1) physiologic measurements of fluid balance, kidney function, and AVP release and sensitivity; (2) behavioral analyses of drinking and motivation in response to diverse thirst stimuli (food, dehydration, hyperosmolality, and hypovolemia); (3) neural recordings from circuit nodes that control drinking (SFO^{Glut}), AVP release (PVH^{AVP} neurons), and motivation (dopamine release in nucleus accumbens), and (4) optogenetic manipulations to test the sufficiency of circuit nodes. These experiments revealed that a subset of these functions is impaired during aging, whereas others are unexpectedly enhanced. These findings provide for the first time a comprehensive view of how a homeostatic system is altered by the aging process and lays the groundwork for targeted interventions to combat dehydration in the elderly.

RESULTS

Aged mice are chronically dehydrated and have renal dysfunction

We set out to characterize how aging affects fluid homeostasis in the mouse. We first measured plasma osmolality in mice of different ages (spanning 2 to 30 months) that had *ad libitum* access to food and water. We found that plasma osmolality was elevated in male mice beginning at 26 months of age (312 ± 4 vs. 330 ± 2 mOsm/kg, 2-5 mo. vs. 26 mo., P = 0.005, **Fig 1c**) and in female mice at 30 months of age (318 ± 3 vs. 339 ± 7 mOsm/kg, 2-5 mo. vs. 26 mo., P < 0.001, **Fig 1c**). Of note, 26-30 months in

bioRxiv preprint doi: https://doi.org/10.1101/2024.09.26.615271; this version posted September 27, 2024. The copyright holder for this preprint (which was not certified by peer review) is the author/funder, who has granted bioRxiv a license to display the preprint in perpetuity. It is made available under aCC-BY-NC-ND 4.0 International license.

the mouse corresponds to 73 - 81 years of age in humans[19], indicating that in mice, as in humans, aging is associated with chronic dehydration.

Fluid homeostasis is governed by two primary mechanisms: water consumption (drinking) and water loss from the kidney. We first characterized renal function in aging mice. We found that aging was associated with reduced urine osmolality, indicating a potential defect in water resorption, in both male (2201 ± 80 vs. 1716 ± 74 mOsm/kg, 2-5 mo. vs. 26 mo., P = 0.0042, **Fig 1d**) and female mice (2500 ± 90 vs. 1864 ± 123 mOsm/kg, 2-5 mo. vs. 26 mo., P = 0.0001, **Fig 1d**). Consistently, urine volume was increased with age in male (12.3 ± 0.9 vs. 16.7 ± 0.7 µL/g BW, 2-3 mo. vs. 26 mo., P = 0.0134, **Fig 1e**) and female mice (14.7 ± 0.7 vs. 23.5 ± 2.4 µL/g, 2-5 mo. vs. 26 mo., P = 0.0028, **Fig 1e**). This suggests that the dehydration in aging mice may be caused, in part, by decreased renal function.

Renal water absorption is controlled by the hormone vasopressin (AVP), and increased urine volume could be caused by either AVP deficiency or resistance to AVP in the kidney. To determine whether AVP levels are reduced in old mice, we measured AVP concentration in the urine (which directly correlates with plasma AVP levels[20,21] and found that AVP levels were significantly lower in aged mice (male: 665 ± 91 vs. 409 ± 60 pg/mL, 3-5 mo. vs. 26 mo male, P = 0.0301; female: 1296 ± 222 vs. 715 ± 131 pg/mL 3-5 mo. vs. 26 mo female, P = 0.0404, **Fig 1g**). Of note, this AVP deficiency was observed despite the fact that old mice are chronically dehydrated (**Fig. 1c**), which should cause elevated AVP levels.

To determine whether there is also AVP resistance in old animals, we challenged mice with a high dose of desmopressin (dDAVP), a selective agonist of the AVP V2 receptor that is expressed in the kidney[22,23], thereby maximally activating renal AVP signaling. We found that dDAVP significantly increased urine osmolality (reflecting enhanced urine concentrating ability) in both young and old mice (**Fig 1f**). However, aged mice still displayed lower urine osmolality than young controls four hours after dDAVP treatment (male: 3523 ± 68 vs. 2389 ± 117 mOsm/kg, young vs. aged, P < 0.0001; female: 3382 ± 126 vs. 2539 ± 201 mOsm/kg, young vs. aged, P < 0.0001, **Fig 1f**), indicating a relative resistance to AVP. Taken together, these data show that aged mice are chronically dehydrated and that this involves a combination of AVP deficiency and resistance.

Aging alters the response of AVP neurons to eating and drinking

AVP is produced by neurosecretory cells located in the paraventricular hypothalamus (PVH) and supraoptic nucleus (SON). Given that circulating AVP levels are reduced with aging in mice **(Fig 1g**),

bioRxiv preprint doi: https://doi.org/10.1101/2024.09.26.615271; this version posted September 27, 2024. The copyright holder for this preprint (which was not certified by peer review) is the author/funder, who has granted bioRxiv a license to display the preprint in perpetuity. It is made available under aCC-BY-NC-ND 4.0 International license.

we investigated whether the activity of PVH^{AVP} neurons during eating and drinking is also altered in old animals.

We prepared mice for fiber photometry recordings of PVH^{AVP} neurons by injecting a Cre-dependent AAV expressing the calcium indicator GCaMP6s into the PVH of $AVP^{Cre/+}$ male mice and, in the same surgery, implanted an optical fiber above the PVH (**Fig 2a, b**). Because consumption of dry food is a primary stimulus for AVP secretion in rodents[17,24], we measured AVP neuron responses to food consumption. Mice were fasted overnight and then provided dry chow for 30 min (without water) followed by water access for 30 min without chow (**Fig. 2c**). We found that PVH^{AVP} neurons were gradually activated during chow consumption in both young and old mice[17,24] (**Fig. 2d**). However, this AVP activation was significantly slower in old male mice compared to young controls (time to half max, 13.7 ± 1.0 vs. 18.3 ± 0.9 min, young vs. aged, P = 0.006, **Fig 2e**) and the magnitude of activation over the entire trial was reduced (mean z score: 1.06 ± 0.11 vs. 0.76 ± 0.07 z, young vs. aged, P = 0.04, **Fig 2g**). Moreover, examination of the microstructure of feeding revealed that young mice exhibited spikes in AVP activity after feeding bouts terminated, while these spikes were reduced in old animals (**Fig. 2i, j**). These differences in neural activity are unlikely to be due to differences in behavior, because there was no difference between young and old animals in the latency to initiate feeding (36.3 ± 6.4 vs. 37.5 ± 3.1 sec, young vs. aged, P = 0.87, **Fig 2f**) or in the amount of chow consumed during the trial (0.37 ± 0.02 vs. 0.37 ± 0.06 g, young vs. aged, P = 0.97, **Fig 2h**). Thus, aged male mice show decreases in AVP neuronal responses to food.

AVP neurons are rapidly inhibited by ingestion of water[17,24]. When given water after food, young and old mice both engaged in drinking (**Fig 2d, k**) and PVH^{AVP} neurons were inactivated to a similar extent (-1.8 ± 0.3 vs. -1.6 ± 0.4 z, young vs. aged, P = 0.62, **Fig 2k, n**). This inactivation was slower in aged compared to young controls (1.3 ± 0.2 vs. 2.5 ± 0.5 min, young vs. aged, P = 0.01, **Fig 2l**), but there was also a trend toward slower water intake in aged animals (mean lick rate: 2.9 ± 0.5 vs. 1.8 ± 0.9 Hz, young vs. aged, P = 0.11, **Fig 2m**), which potentially confounds interpretation of neural activity differences. To better understand this drinking phenotype, we investigated next how water intake is altered with age.

Drinking after eating bouts is delayed in aged mice

Rodents, like humans, consume most of their water during meals[25–29]. We therefore investigated the dynamics of eating and drinking in aged mice with *ad libitum* access to dry food and water (**Fig 3a**). Because prior studies of eating and drinking in old rodents had limited temporal resolution and were

bioRxiv preprint doi: https://doi.org/10.1101/2024.09.26.615271; this version posted September 27, 2024. The copyright holder for this preprint (which was not certified by peer review) is the author/funder, who has granted bioRxiv a license to display the preprint in perpetuity. It is made available under aCC-BY-NC-ND 4.0 International license.

only performed in males[30–32], we used an automated food dispenser and lickometer system to record intake behavior over days at subsecond resolution in both male and female mice at young (3-5 mo) and old (26-27 mo) ages.

We observed no significant difference in the total amount of food and water consumed per day in young and old mice (**Extended Data Fig 2a**). Because water intake is highly sensitive to the amount of dry food consumed, we also normalized water intake to the amount of food intake, which also showed no significant age-related changes on a timescale of 24 hours (**Extended Data Fig 2a**). This indicates there are no gross changes in total water consumption per day in aged animals. However, it is important to note that because aged animals are chronically dehydrated (**Fig 1a**) and also have a failure to appropriately concentrate their urine and retain water (**Fig 1d, e**), this level of intake represents a failure to adjust drinking behavior to match physiologic need.

We wondered whether young and old animals might show differences in their temporal patterns of eating and drinking. To probe this, we analyzed the relationship between consumption of food pellets and subsequent initiation of drinking (**Fig 3a, b**). We found that young mice exhibited a tight temporal coupling between food and water intake, whereas in aged mice the latency between pellet retrieval and the subsequent lick bout was significantly increased (male: 4.0 ± 0.5 vs. 21.3 ± 14.0 min, young vs. aged, P = 0.008; female: 3.5 ± 0.4 vs. 4.5 ± 0.2 min, young vs. aged, P = 0.0062, **Fig 3c, d**). Of note, when old mice did initiate drinking, the lick bouts were larger and longer than in young animals, possibly to compensate for delayed bout initiation (**Extended Data Fig 2d-f**). Thus, aged mice have a specific defect in the short-timescale temporal coupling between eating and drinking.

Food intake and SFO activity are uncoupled on short timescales in aged mice

The age-related delay in water consumption following food ingestion could be due to (1) a delayed activation of primary thirst circuits or (2) delayed responses in downstream cells. To distinguish between these possibilities, we monitored the activity of SFO^{Glut} neurons, which are primary sensory neurons that are activated by food consumption and promote thirst[1,14,16,33,34] . We prepared mice for fiber photometry recordings of SFO^{Glut} neurons (**Fig 3e, h**), fasted mice overnight and then provided access to dry chow without water and recorded responses (**Fig 3f, g**). Similar to PVH^{AVP} neurons, we observed a ramping activation of SFO^{Glut} neurons over ~10 min during eating (**Fig 3i, k**). Examination of the short timescale relationship between individual feeding bouts and SFO-Glut activity revealed that young mice consistently showed a spike in SFO activity after feeding bouts terminated, whereas old mice showed no change (**Fig 3i-l**). This difference mirrors the disrupted short timescale coupling

bioRxiv preprint doi: https://doi.org/10.1101/2024.09.26.615271; this version posted September 27, 2024. The copyright holder for this preprint (which was not certified by peer review) is the author/funder, who has granted bioRxiv a license to display the preprint in perpetuity. It is made available under aCC-BY-NC-ND 4.0 International license.

between eating and neural activity we observed in PVH^{AVP} neurons (**Fig 2i, j**). Thus, the delayed onset of drinking after feeding in old mice (**Fig 3d**) may be due to defective SFO activation in response to acute (i.e. presystemic) ingestive signals.

In contrast to these short timescale differences, we observed no difference between young and old animals in the total amount of food consumed (**Fig 4a-c**), the magnitude of SFO^{Glut} neuronal activation over the entire trial (**Extended Data Fig 3f**), or the time to half maximal SFO^{Glut} activation in males (**Extended Data Fig 3d**) indicating that SFO^{Glut} neurons respond similarly to food ingestion in young and old animals on a timescale of ~30 min. When aged females (but not males) were given reaccess to water (Fig 4a, b), we did observe that they drank less than young animals (859 ± 86 vs. 409 ± 56 licks, young vs. aged, P <0.001, **Fig 4d**) and we confirmed this result with a second cohort of mice (**Extended Data Fig 3m, n**). Consistent with this behavior, the magnitude of SFO^{Glut} inhibition by water drinking was smaller in aged females compared to young females (**Fig 4i**). However, we are hesitant to ascribe this effect to an age-related decline in thirst, because the difference was driven by unusually high water intake in the young female mice, which exceeded that of young males (859 ± 86 vs. 443 ± 54 licks, female vs. male, P < 0.001, unpaired t-test). This suggests that young female mice show a specific enhancement in prandial thirst, which is lost during aging. In addition, there was a trend toward slower SFO^{Glut} inhibition in aged compared to young controls (male: 2.5 ± 0.2 vs. 3.4 ± 0.3 min, P = 0.04; female: 2.8 ± 0.2 vs. 3.2 ± 0.2, P = 0.12, young vs. aged**, Fig 4g**), but this could be confounded by slower water intake in aged animals (mean lick rate, male: 1.8 ± 0.2 vs. 1.3 ± 0.1 Hz, young vs. aged, P = 0.02; female: 3.9 ± 0.5 vs. 1.7 ± 0.3, P = 0.004, young vs. aged, **Fig 4h**).

Water intake after deprivation increases with age

The preceding data show that aging alters primarily the short timescale coupling between eating and drinking, which is determined by pre-systemic cues from the oropharynx and GI tract[1,33,35–38]. To characterize how aging alters responses to systemic signals, we first measured the response of young and old mice to 24-hour water deprivation. We found that water deprivation increased blood osmolality in both young and old mice, but there was no difference in the absolute blood osmolality after deprivation between young and old animals (**Fig 5a**). This was despite the fact that aged mice had a higher starting blood osmolality (**Fig 5a**) and a reduced capacity to concentrate their urine (**Fig 5b**). It is possible that these defects in old mice were compensated for by opposing changes in urine volume, water loss by other routes, or food intake during the 24-hour deprivation.

bioRxiv preprint doi: https://doi.org/10.1101/2024.09.26.615271; this version posted September 27, 2024. The copyright holder for this preprint (which was not certified by peer review) is the author/funder, who has granted bioRxiv a license to display the preprint in perpetuity. It is made available under aCC-BY-NC-ND 4.0 International license.

We next measured water intake when mice were given re-access to water for 30 min following 24-hour deprivation (**Fig 5c**). Surprisingly, we found that aged male and female mice consumed more water than their young counterparts in this test (male: 489 ± 36 vs. 795 ± 93 licks, young vs. aged, P = 0.01; female: 463 ± 66 vs. 722 ± 46 licks, young vs. aged, P = 0.005, **Fig 5d**). This difference persisted when we normalized the water intake to the body surface area (male: 66.2 ± 5.8 vs. 101.4 ± 12.5 mg/g$^{0.667}$, young vs. aged, P = 0.04; female: 62.3 ± 3.2 vs. 108.9 ± 8.6 mg/g$^{0.667}$, young vs. aged, P < 0.001, **Fig 5i**), which has been proposed as a method to correct for differences between animals in body size[16,17]. Thus, although the plasma osmolality of young and old mice is similar after 24-hour deprivation, old mice drink more when water is again made available.

We considered two hypotheses, which are not mutually exclusive, for why aged mice would drink more after water deprivation. The first possibility is that there is a defect in thirst satiation in old animals. Thirst satiation is encoded in the inhibition of SFO^{Glut} neurons, which show stepwise decreases in activity during drinking that track the volume of fluid consumed[18]. If aged mice have a defect in thirst satiation, then we would expect SFO^{Glut} neurons to be inhibited more slowly when old mice drink. Indeed, we observed that SFO^{Glut} neurons showed a delayed inhibition when old male mice drank after 24-hour deprivation (time to half decline: 1.5 ± 0.2 vs. 2.4 ± 0.2 min, young vs. aged, P = 0.008, **Fig 5f**), and a similar trend was observed in old females (2.0 ± 0.2 vs. 2.4 ± 0.2 min, young vs. aged, P = 0.26, **Fig 5f**). The difference was only observed in the kinetics, because the magnitude of SFO^{Glut} inhibition by water drinking was similar in young and aged mice (**Fig 5e, h**). Importantly, this difference was not due to differences in behavior, because young and old mice drank at the same rate when water was made first available (**Fig 5g**). This suggests that the overdrinking of old mice may be caused, in part, by an age-related impairment in the presystemic sensory feedback that inhibits SFO^{Glut} neurons during water consumption.

Functional manipulations suggest greater SFO activation in aged animals after deprivation

An alternative, and not mutually exclusive, explanation for why aged animals drink more after water deprivation is that the thirst circuitry is activated more strongly. In this regard, while photometry can measure relative changes in response to a stimulus, it cannot reliably quantify absolute differences in activity between cohorts of animals. Thus, it is possible that aged animals, despite similar blood osmolality as young animals, have greater activation of the thirst circuitry after water deprivation and this causes them to drink more.

bioRxiv preprint doi: https://doi.org/10.1101/2024.09.26.615271; this version posted September 27, 2024. The copyright holder for this preprint (which was not certified by peer review) is the author/funder, who has granted bioRxiv a license to display the preprint in perpetuity. It is made available under aCC-BY-NC-ND 4.0 International license.

We performed three sets of experiments to test this hypothesis. First, we took advantage of the fact that optogenetic stimulation of SFO^{Glut} neurons creates a state of virtual thirst that drives drinking in water-sated animals[14-15,18,41,42]. Therefore, by optogenetic stimulation of SFO^{Glut} neurons, we can introduce a fixed amount of activation into the thirst circuit of young and old animals and then compare the behavioral responses. We targeted ChR2 to SFO^{Glut} neurons of young and old male mice by viral injection of a Cre-dependent AAV and implanted an optical fiber above the SFO (**Fig 6a**). We first water-deprived these animals for 24 hours and then measured intake for 30 min in the absence of laser stimulation. Old mice showed a clear trend toward consuming more water than young animals after 24-hour deprivation (386 ± 61 vs. 845 ± 284 licks, young vs. aged, P = 0.08, **Fig 6c**), mirroring our findings from a different cohort of mice used for photometry experiments (**Fig 5d**). We then optogenetically stimulated the same animals, while water sated, and measured drinking (**Fig 6b**). Strikingly, we found that there was no difference in the amount of water consumed between young and old animals after artificial activation of the SFO^{Glut} (757 ± 212 vs. 662 ± 385 licks, young vs. aged, P = 0.84, unpaired t-test, **Fig. 6d**). The fact that we observe no difference in this test is consistent with the hypothesis that the greater water consumption in aged animals is due to greater activation of this circuitry following 24-hour deprivation.

To test this hypothesis a second way, we asked whether there are differences between young and old animals in their motivation to work for water. We reasoned that if aged mice drink more because they have greater SFO activation, then they should also lever press more in an operant task for water, since this is controlled by SFO activity[42,43]. On the other hand, if aged mice drink more primarily because they have a reduced rate of thirst satiation (i.e. delayed SFO inhibition during drinking), then they should not lever press more, because satiation is typically not achieved in an operant task due to the reduced total consumption.

We trained mice on a fixed-ratio 1 (FR1) schedule, so that they received one drop of water for each press of the active lever but not the inactive lever (**Fig. 7a**). We then water-deprived animals for 24 hours and measured lever pressing in a 30 min test. Strikingly, we found that aged male and female mice both engaged in more lever pressing for water compared to young controls (male: 55 ± 6 vs. 89 ± 9, young vs. aged, P = 0.02, female: 49 ± 5 vs. 73 ± 7, young vs. aged, P = 0.04, **Fig. 7b, c**). This enhanced responding was specific to the active lever, confirming that old mice have heightened motivation specifically for water. Importantly, both young and old mice consumed significantly less water during the FR1 test compared to free drinking (**Extended Data Fig 7a, b**), implying that differences in satiation are unlikely to explain this difference in lever pressing. To exclude any

bioRxiv preprint doi: https://doi.org/10.1101/2024.09.26.615271; this version posted September 27, 2024. The copyright holder for this preprint (which was not certified by peer review) is the author/funder, who has granted bioRxiv a license to display the preprint in perpetuity. It is made available under aCC-BY-NC-ND 4.0 International license.

contribution from differences in satiation, we performed a progressive ratio test (PR3) in which animals were required to perform an increasing number of lever presses for each subsequent water reward, such that they reach a “break point" long before their thirst has been significantly reduced. In this test, we observed again that old male mice lever pressed more vigorously than young controls (break point: 8 ± 1 vs. 15 ± 2, young vs. aged, P = 0.02, **Fig 7d**). In females, there was a trend to greater lever pressing that was non-significant (8 ± 1 vs. 10 ± 1, young vs. aged, P = 0.33, **Fig 7d**). Together, these data show that aged mice show increased motivation for water following 24-hour deprivation, consistent with stronger activation of thirst circuitry in this context.

Motivation for water is controlled, in part, by dopamine release in the nucleus accumbens (NAc). Cues that predict water, including its taste, trigger a burst of DA in NAc that helps to orient and energize further actions toward obtaining water[44–46]. The magnitude of this DA release is controlled by SFO^{Glut} neuron activity and is greater in thirsty animals[45,46]. We therefore measured water-triggered DA release in NAc as an independent measure of whether old animals have greater activation of the thirst circuitry following 24-hour deprivation.

We targeted the genetically encoded DA sensor GRAB-DA3m to the NAc and, in the same surgery, implanted an optical fiber above the NAc to record DA release by fiber photometry (**Fig. 7e**). Mice were water deprived for 24 hours and then given access to a water bottle for self-paced drinking. The onset of drinking was accompanied by a spike in DA release in both young and old animals, but this increase was bigger (**Extended Data Fig 7d**) and lasted longer (time to half decline, male: 38.1 ± 3.3 vs. 74.8 ± 17.4 s, P = 0.03; female: 35.2 ± 2.8 vs. 66.2 ± 10.4 s, P = 0.007, **Extended Data Fig 7e**) in aged mice. In contrast, there was no difference in the DA response when young and old mice were presented with an empty water bottle, indicating that this effect is specific to water (**Extended Data Fig 7f, g**). Of note, aged mice drank more water during the 30 min test after deprivation (**Extended Data Fig 7c**), as observed previously (**Fig 5d**), but differential DA release was observed even at early time points (i.e. 1 minute from the onset of drinking bout) (male: 1.47 ± 0.20 vs. 2.15 ± 0.24 z, young vs. aged, P = 0.05; female: 1.13 ± 0.23 vs. 2.35 ± 0.15 z, young vs. aged, P < 0.001, **Fig 7f, h**) when the amount drunk was similar (male: 304 ± 20 vs. 318 ± 41 licks, young vs. aged, P = 0.76; female: 185 ± 9 vs. 211 ± 10 licks, young vs. aged, P = 0.08, **Fig 7g**), indicating that this cannot be attributed to differences in behavior. Taken together, these results show that, following 24-hour water deprivation, aged mice drink more (**Fig 5d**; **Extended Data Fig 7c**), show greater motivation to work for water (**Fig 7b-d**), and show greater water-triggered DA release in NAc (**Fig 7h**). This strongly argues that the core thirst circuitry is more strongly activated following 24-hour deprivation in aged mice.

bioRxiv preprint doi: https://doi.org/10.1101/2024.09.26.615271; this version posted September 27, 2024. The copyright holder for this preprint (which was not certified by peer review) is the author/funder, who has granted bioRxiv a license to display the preprint in perpetuity. It is made available under aCC-BY-NC-ND 4.0 International license.

Aged mice have intact water consumption and delayed SFO-Glut inhibition after osmotic thirst

Water deprivation results in increased blood osmolality and decreased blood volume, both of which promote thirst. To characterize how these two pathways are altered by age, we independently manipulated them and measured drinking behavior and SFO^{Glut} neuronal responses.

We first investigated the role of blood osmolality by giving mice an intraperitoneal injection of hypertonic saline (2 M), which increases plasma osmolality without significantly altering blood volume[47]. Salt injection activated SFO^{Glut} neurons in young and old mice to a similar extent (**Fig 8c, Extended Data Fig 8c**), and with similar kinetics (**Extended Data Fig 8b**). We then made water available and recorded responses during 30 min of self-paced drinking (**Fig 8a, d-g**). In contrast to 24-hour deprivation, we observed no significant age-related differences in water intake in either male (756 ± 93 vs. 784 ± 135 licks, young vs. aged, P = 0.8, **Fig 8b**) or female mice (875 ± 94 vs. 1065 ± 185 licks young vs. aged, P = 0.33, **Fig 8b**). We replicated this finding in a separate cohort of young and old mice (**Extended Data Fig 8d, e**). However, when we examined SFO^{Glut} neuronal recordings, we found that the activity of these neurons during drinking declined more slowly in aged animals (male: 2.4 ± 0.4 vs. 6.4 ± 1.1 min, young vs. aged, P = 0.009; female: 1.8 ± 0.2 vs. 4.4 ± 1.0 min young vs. aged, P = 0.02, **Fig 8e**). This was not due to differences in lick rate in young and old animals (**Fig 8f**) and mirrors the finding of slower SFO^{Glut} inhibition when old animals drink after 24-hour deprivation (**Fig 5f**). Together, these data indicate that, in aged animals, SFO^{Glut} neurons are able to sense changes in blood osmolality appropriately, but that there is a delay in their inhibition by presystemic cues during drinking.

Water consumption after hypovolemia is selectively reduced in aged females

We next investigated how aging affects responses to decreases in blood volume. To do this, we used a paradigm[48] in which mice are given subcutaneous injection of polyethylene glycol (PEG), which forms an edema under the skin that draws water out of the circulation and thereby reduces blood volume. We found that PEG injection resulted in a ramping activation of SFO^{Glut} neurons, and there was no difference in the magnitude or rate of this activation in young versus old mice (**Fig 8j, Extended Data Fig 8i, j**). When mice were subsequently given reaccess to water for 30 min (**Fig 8h, k-n**), we found old females, but not males, consumed much less water than their young counterparts (**Fig 8i**), which we confirmed in an independent cohort of young and old mice (**Extended Data Fig 8k, l**). Interestingly, these differences between young and old female mice were driven by unusually high intake in the young females, which exceeded that in young males (433 ± 34 vs. 241 ± 47 licks, female vs. male, P =

bioRxiv preprint doi: https://doi.org/10.1101/2024.09.26.615271; this version posted September 27, 2024. The copyright holder for this preprint (which was not certified by peer review) is the author/funder, who has granted bioRxiv a license to display the preprint in perpetuity. It is made available under aCC-BY-NC-ND 4.0 International license.

0.006, unpaired t-test, **Fig 8i**). This mirrors what we observed in assays of prandial thirst (**Fig 4d**), in which young females consumed much more water than other cohorts. This suggests that food intake and PEG-induced hypovolemia, but not other dipsogenic stimuli, may act through a common mechanism that causes overdrinking in young females. One candidate mechanism is the hormone Angiotensin II (AngII), which is implicated in both prandial drinking and hypovolemia[18,49–51], but we did not observe a difference between young and old animals in the SFO^{Glut} response to an injection of AngII (**Extended Data Fig 4a, c**).

DISCUSSION

Deterioration of fluid homeostasis is one of the hallmarks of aging, but the underlying causes are not well understood. In this study, we have systematically investigated how aging alters fluid balance in the mouse, comparing young and old animals of both sexes across a range of physiologic, behavioral, and neural circuit analyses. This has revealed that aging induces a complex, but reproducible, constellation of fluid homeostasis phenotypes in the mouse. These include (1) chronic dehydration that begins at 26-30 months of age, (2) decreased water resorption by the kidney, secondary to both AVP deficiency and resistance, (3) impaired short-timescale coupling between eating and drinking, both behaviorally and at the level of neural dynamics, (4) delayed inhibition of thirst circuits during drinking, and, surprisingly, (5) an increase in water intake, as well as thirst motivation, in old animals after 24-hour water deprivation, but not in response to any other dipsogenic stimuli.

Aged mice have a primary defect in AVP signaling

We found that old mice of both sexes exhibited chronic dehydration, and this was accompanied by consistent deficits in AVP secretion and function. These deficits included (1) dilute urine, indicating a reduced ability of the kidney to concentrate urine, (2) reduced AVP levels, despite blood hyperosmolality, and (3) reduced ability to concentrate urine in response to supraphysiologic AVPR stimulation, indicating AVP resistance. Because the defects in fluid consumption we observed were mostly acute in nature (discussed below), this suggests that the dehydration in aged mice is driven primarily by deterioration of the AVP-kidney axis.

Previous studies have reported mixed findings on the effect of aging on AVP function in different species. Most studies have been performed in rats, where it has been reported that old animals have fewer AVP cells in the PVH and reduced expression of AVP[52,53]. While some studies report reduced

bioRxiv preprint doi: https://doi.org/10.1101/2024.09.26.615271; this version posted September 27, 2024. The copyright holder for this preprint (which was not certified by peer review) is the author/funder, who has granted bioRxiv a license to display the preprint in perpetuity. It is made available under aCC-BY-NC-ND 4.0 International license.

circulating levels of AVP[52], others have found old animals have normal or even enhanced levels of AVP in the blood[53,55,56]. Similar variability has been found in humans[6,57–59]. These differences could have many causes, including the age of the animals (we used 26-30 month-old mice, which are older than the animals used in many studies); the species, strain, and sex; and the diet on which the animals are maintained over the lifetime. Although we cannot reconcile all these differences, our findings establish a baseline for how aging effects AVP and kidney function in the C57BL/6 mouse strain, which is a commonly used model organism for aging research.

Aging primarily impairs responses to presystemic thirst signals

The signals that control thirst are traditionally divided into two classes: (1) systemic signals that arise from the blood (i.e. hyperosmolality and hypovolemia,) and which are primarily involved in generating thirst after water deprivation[1,35,60], and (2) presystemic signals that arise from the oropharynx and gastrointestinal (GI) tract which are primarily involved in the rapid control of thirst by ingestion (i.e. the quenching of thirst during drinking and the stimulation of thirst during eating)[1,35,37–39]. A basic answered question regards how these two classes of signals are differentially affected by aging.

We examined the response of young and old mice to presystemic and systemic thirst signals at the level of both behavior and neural circuit dynamics. The general finding from these experiments was that old mice show evidence of impaired responses to ingestion (eating and drinking) but not to manipulations of the blood. For example, aged mice had a consistent delay in the short timescale coupling between eating food and subsequent water intake, and this delay was accompanied by altered neural dynamics during eating for both PVH^{AVP} and SFO^{Glut} neurons (**Fig 2j, 3j, 3l**). There was also an impairment in the rapid inhibition of PVH^{AVP} and SFO^{Glut} neurons during drinking, such that this inhibition was slower (**Fig 2l, 4g, 5f, Extended Data Fig 5e**) and less efficient (i.e. reduced Δ z per lick; **Extended Data Fig 3l, 6e**). In some experiments, these impairments may have contributed to overdrinking in aged animals (**Fig 5d**). The magnitude of these acute defects was moderate, and in most cases aged animals were able to compensate by adjusting behavior on longer timescales (e.g. **Extended Data Fig 2a**). Nonetheless, we observed these changes across multiple cohorts of aged mice of both sexes, suggesting that they are a general feature of aging of the fluid homeostasis system. Of note, because presystemic signals are detected by sensory innervation of the mouth, throat, and GI tract, these changes could reflect the age-dependent deterioration of these primary sensory afferents. This would mirror the well-known age-dependent changes in primary sensory neurons in other sensory systems, such as vision and hearing[61,62].

bioRxiv preprint doi: https://doi.org/10.1101/2024.09.26.615271; this version posted September 27, 2024. The copyright holder for this preprint (which was not certified by peer review) is the author/funder, who has granted bioRxiv a license to display the preprint in perpetuity. It is made available under aCC-BY-NC-ND 4.0 International license.

In contrast, we saw little difference between young and old animals following direct manipulations of the blood. Thus, young and old mice of both sexes responded normally to increases in blood hyperosmolality, both in terms of the amount of water consumed (**Fig 8b**) and the response to SFO^{Glut} neurons (**Fig 8b-c**). For hypovolemia, we observed normal responses in aged male mice (**Fig 8i**), whereas aged females consistently consumed less water than young animals. However, as noted in the text, we are hesitant to ascribe this to an age-dependent defect, because the difference arose from exaggerated fluid intake in the young females when compared to males of the same age. One possible explanation for this observation is that it reflects an adaption of the fluid homeostasis system to the demands of reproduction, which results in an increase in bodily fluid volume of 45% during pregnancy[63–65]. This may make female mice of reproductive-age hypersensitive to signals of hypovolemia.

Aged mice show unexpectedly enhanced thirst after water deprivation

A surprising result from our experiments was that aged male and female mice consumed more water than young animals after 24-hour water deprivation (**Fig 5d**). This consistent result was accompanied by increased motivation to work for water (**Fig 7b-d**) and increased dopamine release in NAc in response to water consumption (**Fig 7h**), suggesting that aged mice have greater activation of the thirst circuit after 24-hour deprivation. This is at odds with the general observation that aged animals show reduced thirst, and indeed our finding that old mice are chronically dehydrated (**Fig 1c, d**). It also appears inconsistent with our finding that old animals do not overdrink in response to isolated blood hyperosmolality or hypervolemia (**Fig 8b, i**).

How can we explain these findings? The simplest explanation is that 24-hour water deprivation causes substantially greater dehydration in old mice than young animals. This would be predicted from the fact that old animals have decreased AVP function and impaired urine concentrating ability (**Fig 1b-g**), and, for this reason, it was surprising that we observed similar blood osmolality in young and old animals after 24-hour water deprivation (**Fig 5a**). However, it is possible that measurements of blood volume, which we were unable to perform in this experiment, would have revealed a greater deficit in old animals. Alternatively, if thirst is influenced by the duration of blood hyperosmolality, then the fact that old animals likely become dehydrated faster in response to water deprivation may be important. Addressing these questions will require measuring the timecourse of blood osmolality and volume following water deprivation in young and old animals and correlating this with behavioral and neural endpoints.

bioRxiv preprint doi: https://doi.org/10.1101/2024.09.26.615271; this version posted September 27, 2024. The copyright holder for this preprint (which was not certified by peer review) is the author/funder, who has granted bioRxiv a license to display the preprint in perpetuity. It is made available under aCC-BY-NC-ND 4.0 International license.

REFERENCES

1. Zimmerman, C. A., Leib, D. E. & Knight, Z. A. Neural circuits underlying thirst and fluid homeostasis. *Nat Rev Neurosci* **18**, 459–469 (2017).

2. Phillips, P. A. *et al.* Reduced Thirst after Water Deprivation in Healthy Elderly Men. *N Engl J Med* **311**, 753–759 (1984).

3. Miescher, E. & Fortney, S. M. Responses to dehydration and rehydration during heat exposure in young and older men. *American Journal of Physiology-Regulatory, Integrative and Comparative Physiology* **257**, R1050–R1056 (1989).

4. Phillips, P. A., Bretherton, M., Johnston, C. I. & Gray, L. Reduced osmotic thirst in healthy elderly men. *American Journal of Physiology-Regulatory, Integrative and Comparative Physiology* **261**, R166–R171 (1991).

5. Mack, G. W. *et al.* Body fluid balance in dehydrated healthy older men: thirst and renal osmoregulation. *Journal of Applied Physiology* **76**, 1615–1623 (1994).

6. Davies, I., O'Neill, P. A., Mclean, K. A., Catania, J. & Bennett, D. Age-associated Alterations in Thirst and Arginine Vasopressin in Response to a Water or Sodium Load. *Age Ageing* **24**, 151–159 (1995).

7. Stachenfeld, N. S., Mack, G. W., Takamata, A., DiPietro, L. & Nadel, E. R. Thirst and fluid regulatory responses to hypertonicity in older adults. *American Journal of Physiology-Regulatory, Integrative and Comparative Physiology* **271**, R757–R765 (1996).

8. Zappe, D. H., Bell, G. W., Swartzentruber, H., Wideman, R. F. & Kenney, W. L. Age and regulation of fluid and electrolyte balance during repeated exercise sessions. *American Journal of Physiology-Regulatory, Integrative and Comparative Physiology* **270**, R71–R79 (1996).

9. Takamata, A. *et al.* Effect of an exercise-heat acclimation program on body fluid regulatory responses to dehydration in older men. *American Journal of Physiology-Regulatory, Integrative and Comparative Physiology* **277**, R1041–R1050 (1999).

10. Tamma, G., Goswami, N., Reichmuth, J., De Santo, N. G. & Valenti, G. Aquaporins, Vasopressin, and Aging: Current Perspectives. *Endocrinology* **156**, 777–788 (2015).

bioRxiv preprint doi: https://doi.org/10.1101/2024.09.26.615271; this version posted September 27, 2024. The copyright holder for this preprint (which was not certified by peer review) is the author/funder, who has granted bioRxiv a license to display the preprint in perpetuity. It is made available under aCC-BY-NC-ND 4.0 International license.

11. Stookey, J. D., Pieper, C. F. & Cohen, H. J. Is the prevalence of dehydration among community-dwelling older adults really low? Informing current debate over the fluid recommendation for adults aged 70+years. *Public Health Nutr.* **8**, 1275–1285 (2005).

12. Dmitrieva, N. I., Gagarin, A., Liu, D., Wu, C. O. & Boehm, M. Middle-age high normal serum sodium as a risk factor for accelerated biological aging, chronic diseases, and premature mortality. *eBioMedicine* **87**, 104404 (2023).

13. El-Sharkawy, A. M., Sahota, O., Maughan, R. J. & Lobo, D. N. The pathophysiology of fluid and electrolyte balance in the older adult surgical patient. *Clinical Nutrition* **33**, 6–13 (2014).

14. Oka, Y., Ye, M. & Zuker, C. S. Thirst driving and suppressing signals encoded by distinct neural populations in the brain. *Nature* **520**, 349–352 (2015).

15. Betley, J. N. *et al.* Neurons for hunger and thirst transmit a negative-valence teaching signal. *Nature* **521**, 180–185 (2015).

16. Richter, C. P. & Brailey, M. E. Water-intake and its relation to the surface area of the body. *Proc. Natl. Acad. Sci.* **15**, 570–578 (1929).

17. Tordoff, M. G., Bachmanov, A. A. & Reed, D. R. Forty mouse strain survey of water and sodium intake. *Physiol. Behav.* **91**, 620–631 (2007).

18. Zimmerman, C. A. *et al.* Thirst neurons anticipate the homeostatic consequences of eating and drinking. *Nature* **537**, 680–684 (2016).

19. Mandelblat-Cerf, Y. *et al.* Bidirectional Anticipation of Future Osmotic Challenges by Vasopressin Neurons. *Neuron* **93**, 57–65 (2017).

20. Nation, H. L., Nicoleau, M., Kinsman, B. J., Browning, K. N. & Stocker, S. D. DREADD-induced activation of subfornical organ neurons stimulates thirst and salt appetite. *Journal of Neurophysiology* **115**, 3123–3129 (2016).

21. Flurkey, K., M. Currer, J. & Harrison, D. E. Chapter 20 - Mouse Models in Aging Research. in *The Mouse in Biomedical Research (Second Edition)* (eds. Fox, J. G. et al.) 637–672 (Academic Press, Burlington, 2007). doi:10.1016/B978-012369454-6/50074-1.

22. Matsui, K., Share, L., Wang, B. C., Crofton, J. T. & Brooks, D. P. Effects of Changes in Steady State Plasma Vasopressin Levels on Renal and Urinary Vasopressin Clearances in the Dog*. *Endocrinology* **112**, 2107–2113 (1983).

bioRxiv preprint doi: https://doi.org/10.1101/2024.09.26.615271; this version posted September 27, 2024. The copyright holder for this preprint (which was not certified by peer review) is the author/funder, who has granted bioRxiv a license to display the preprint in perpetuity. It is made available under aCC-BY-NC-ND 4.0 International license.

23. Moses, A. M. Osmotic thresholds for AVP release with the use of plasma and urine AVP and free water clearance. *American Journal of Physiology-Regulatory, Integrative and Comparative Physiology* **256**, R892–R897 (1989).

24. Saito, M., Tahara, A. & Sugimoto, T. 1-desamino-8-d-arginine vasopressin (DDAVP) as an agonist on V1b vasopressin receptor. *Biochemical Pharmacology* **53**, 1711–1717 (1997).

25. Boone, M. & Deen, P. M. T. Physiology and pathophysiology of the vasopressin-regulated renal water reabsorption. *Pflugers Arch - Eur J Physiol* **456**, 1005–1024 (2008).

26. Kim, A., Madara, J. C., Wu, C., Andermann, M. L. & Lowell, B. B. Neural basis for regulation of vasopressin secretion by anticipated disturbances in osmolality. *eLife* **10**, e66609 (2021).

27. Cizek, L. J. & Nocenti, M. R. Relationship between water and food ingestion in the rat. *American Journal of Physiology-Legacy Content* **208**, 615–620 (1965).

28. Kissileff, H. R. Food-associated drinking in the rat. *Journal of Comparative and Physiological Psychology* **67**, 284–300 (1969).

29. Bellisle, F. & Le Magnen, J. The structure of meals in humans: Eating and drinking patterns in lean and obese subjects. *Physiology & Behavior* **27**, 649–658 (1981).

30. De Castro, J. M. A microregulatory analysis of spontaneous fluid intake by humans: Evidence that the amount of liquid ingested and its timing is mainly governed by feeding. *Physiology & Behavior* **43**, 705–714 (1988).

31. Gannon, K. S., Smith, J. C., Henderson, R. & Hendrick, P. A system for studying the microstructure of ingestive behavior in mice. *Physiology & Behavior* **51**, 515–521 (1992).

32. Peng, M. T. & Kang, M. Circadian rhythms and patterns of running-wheel activity, feeding and drinking behaviors of old male rats. *Physiology & Behavior* **33**, 615–620 (1984).

33. Silver, A. J., Flood, J. F. & Morley, J. E. Effect of Aging on Fluid Ingestion in Mice. *Journal of Gerontology* **46**, B117–B121 (1991).

34. Xie, K. *et al.* Every-other-day feeding extends lifespan but fails to delay many symptoms of aging in mice. *Nat Commun* **8**, 155 (2017).

35. Gizowski, C. & Bourque, C. W. The neural basis of homeostatic and anticipatory thirst. *Nat Rev Nephrol* **14**, 11–25 (2018).

bioRxiv preprint doi: https://doi.org/10.1101/2024.09.26.615271; this version posted September 27, 2024. The copyright holder for this preprint (which was not certified by peer review) is the author/funder, who has granted bioRxiv a license to display the preprint in perpetuity. It is made available under aCC-BY-NC-ND 4.0 International license.

36. Fry, M., Hoyda, T. D. & Ferguson, A. V. Making sense of it: roles of the sensory circumventricular organs in feeding and regulation of energy homeostasis. *Exp Biol Med (Maywood)* **232**, 14–26 (2007).

37. Johnson, A. K. & Thunhorst, R. L. The Neuroendocrinology of Thirst and Salt Appetite: Visceral Sensory Signals and Mechanisms of Central Integration. *Frontiers in Neuroendocrinology* **18**, 292–353 (1997).

38. McKinley, M. J. & Johnson, A. K. The Physiological Regulation of Thirst and Fluid Intake. *Physiology* **19**, 1–6 (2004).

39. Stocker, S. D. *et al.* Physiological Mechanisms of Dietary Salt Sensing in the Brain, Kidney, and Gastrointestinal Tract. *Hypertension* **81**, 447–455 (2024).

40. Zimmerman, C. A. *et al.* A gut-to-brain signal of fluid osmolarity controls thirst satiation. *Nature* **568**, 98–102 (2019).

41. Matsuda, T. *et al.* Distinct neural mechanisms for the control of thirst and salt appetite in the subfornical organ. *Nat Neurosci* **20**, 230–241 (2017).

42. Leib, D. E. *et al.* The Forebrain Thirst Circuit Drives Drinking through Negative Reinforcement. *Neuron* **96**, 1272-1281.e4 (2017).

43. Allen, W. E. *et al.* Thirst regulates motivated behavior through modulation of brainwide neural population dynamics. *Science* **364**, eaav3932 (2019).

44. Augustine, V. *et al.* Temporally and Spatially Distinct Thirst Satiation Signals. *Neuron* **103**, 242-249.e4 (2019).

45. Hsu, T. M. *et al.* Thirst recruits phasic dopamine signaling through subfornical organ neurons. *Proc. Natl. Acad. Sci. U.S.A.* **117**, 30744–30754 (2020).

46. Grove, J. C. R. *et al.* Dopamine subsystems that track internal states. *Nature* **608**, 374–380 (2022).

47. Pool, A.-H. *et al.* The cellular basis of distinct thirst modalities. *Nature* **588**, 112–117 (2020).

48. Stricker, E. Osmoregulation and volume regulation in rats: inhibition of hypovolemic thirst by water. *American Journal of Physiology-Legacy Content* **217**, 98–105 (1969).

bioRxiv preprint doi: https://doi.org/10.1101/2024.09.26.615271; this version posted September 27, 2024. The copyright holder for this preprint (which was not certified by peer review) is the author/funder, who has granted bioRxiv a license to display the preprint in perpetuity. It is made available under aCC-BY-NC-ND 4.0 International license.

49. Abdelaal, A. E., Mercer, P. F. & Mogenson, G. J. Plasma angiotensin II levels and water intake following β-adrenergic stimulation, hypovolemia, cellular dehydration and water deprivation. *Pharmacology Biochemistry and Behavior* **4**, 317–321 (1976).

50. Kraly, F. S. & Corneilson, R. Angiotensin II mediates drinking elicited by eating in the rat. *American Journal of Physiology-Regulatory, Integrative and Comparative Physiology* **258**, R436–R442 (1990).

51. McKinley, M. J. *et al.* Osmoregulatory fluid intake but not hypovolemic thirst is intact in mice lacking angiotensin. *American Journal of Physiology-Regulatory, Integrative and Comparative Physiology* **294**, R1533–R1543 (2008).

52. Calzá, L., Giardino, L., Velardo, A., Battistini, N. & Marrama, P. Influence of aging on the neurochemical organization of the rat paraventricular nucleus. *J Chem Neuroanat* **3**, 215–231 (1990).

53. Sauvant, J. *et al.* Mechanisms Involved in Dual Vasopressin/Apelin Neuron Dysfunction during Aging. *PLoS ONE* **9**, e87421 (2014).

54. Zbuzek, V. K. & Wu, W.-H. Age-related vasopressin changes in rat plasma and the hypothalamo-hypophyseal system. *Experimental Gerontology* **17**, 133–138 (1982).

55. Greenwood, M. P. *et al.* The effects of aging on biosynthetic processes in the rat hypothalamic osmoregulatory neuroendocrine system. *Neurobiology of Aging* **65**, 178–191 (2018).

56. Birder, L. A., Wolf-Johnston, A. S., Jackson, E. K., Wein, A. J. & Dmochowski, R. Aging increases the expression of vasopressin receptors in both the kidney and urinary bladder. *Neurourology and Urodynamics* **38**, 393–397 (2019).

57. Kirkland, J., Lye, M., Goddard, C., Vargas, E. & Davies, I. PLASMA ARGININE VASOPRESSIN IN DEHYDRATED ELDERLY PATIENTS. *Clinical Endocrinology* **20**, 451–456 (1984).

58. Duggan, J., Kilfeather, S., Lightman, S. L. & O'Malley, K. The Association of Age with Plasma Arginine Vasopressin and Plasma Osmolality. *Age Ageing* **22**, 332–336 (1993).

59. Johnson, A. G., Crawford, G. A., Kelly, D., Nguyen, T. V. & Gyory, A. Z. Arginine Vasopressin and Osmolality in the Elderly. *J American Geriatrics Society* **42**, 399–404 (1994).

60. Bourque, C. W. Central mechanisms of osmosensation and systemic osmoregulation. *Nat Rev Neurosci* **9**, 519–531 (2008).

bioRxiv preprint doi: https://doi.org/10.1101/2024.09.26.615271; this version posted September 27, 2024. The copyright holder for this preprint (which was not certified by peer review) is the author/funder, who has granted bioRxiv a license to display the preprint in perpetuity. It is made available under aCC-BY-NC-ND 4.0 International license.

61. Peelle, J. E. & Wingfield, A. The Neural Consequences of Age-Related Hearing Loss. *Trends in Neurosciences* **39**, 486–497 (2016).

62. Andersen, G. J. Aging and vision: changes in function and performance from optics to perception. *WIRES Cognitive Science* **3**, 403–410 (2012).

63. Pritchard, J. A. Changes in the Blood Volume During Pregnancy and Delivery. *Anesthesiology* **26**, 393–399 (1965).

64. Sanghavi, M. & Rutherford, J. D. Cardiovascular Physiology of Pregnancy. *Circulation* **130**, 1003–1008 (2014).

65. Soma-Pillay, P., Nelson-Piercy, C., Tolppanen, H. & Mebazaa, A. Physiological changes in pregnancy. *CVJA* **27**, 89–94 (2016).

METHODS

Mouse strains

The C57BL/6J (Jackson laboratory, 000664) mouse strain was used. Mice were housed or aged (for aged mice) in the temperature- and humidity-controlled facilities with 12-hr light-dark cycle and ad libitum access to water and standard chow (PicoLab Rodent Diet 20 #5053). AVP-Cre/+ mice were obtained from the Jackson laboratory.

Plasma and urine osmolality

For plasma, blood was collected from cheek vein into the lithium-heparin-coated tube (RAM scientific) and 1,000xg for 10 minutes, and the supernatant was further centrifuged at 10,000 xg for 10 minutes and to remove platelets. Urine was collected by spontaneous voiding or gentle massage of the abdomen, and centrifuged at 1,000 xg for 5 minutes and the supernatant was diluted by 5 times in water. Osmolality was measured using the Vapro 5600 vapor-pressure osmometer (Wescor Instruments).

dDAVP (Desmopressin) injection

bioRxiv preprint doi: https://doi.org/10.1101/2024.09.26.615271; this version posted September 27, 2024. The copyright holder for this preprint (which was not certified by peer review) is the author/funder, who has granted bioRxiv a license to display the preprint in perpetuity. It is made available under aCC-BY-NC-ND 4.0 International license.

dDAVP (Desmopressin, Cayman Chemical #17348) was dissolved in DMSO to make a 3.35 mg/mL stock, kept frozen -20'C and diluted in PBS on the same day for subcutaneous injection at 300 uL s.c./20g BW (1 mg s.c./kg BW). Urine was collected in the baseline state, 2 hours and 4 hours after dDAVP injection for osmolality measurements.

Urine AVP level

Urine AVP levels were measured by the Arg8-Vasopressin ELISA kit from Enzo (ADI-900-017A). The optical density at 450 nm was measured using Biotek H4 Plate Reader.

Void spot assay and measurement of urine volume

Urine volume was measured by spontaneous voiding on a clean paper (Blick Cosmos blotting paper, 10422-1005). A clean housing cage was removed of all bedding materials, food and water, and prepared with a clean paper (16.0 cm x 30.1 cm) cut and taped on the bottom to cover the entire floor, and 2 pieces of bedding and 1 piece of chow on the paper. An individual mouse was placed in the cage and left in the dark, sound-attenuating PVC cabinet (Med Associates Inc, ENV-018V) for 4 hours from 10 AM to 2 PM. After 4 hours, the mouse was returned to its home cage and the paper was imaged by a gel imaging system (ChemiDoc™ MP, Universal Hood II, BioRad) with the Krypton detection setting. The imaged void area was analyzed using the Void Whizzard plugin[3] on ImageJ. The size of the void area on the paper was converted to urine volume by a standard calibration curve with a series of known volumes of urine which had a linear relationship with the size of the urine spot. A spot size corresponding to 0.5 uL of urine or smaller was excluded to avoid nonspecific marks.

Ad libitum feeding and drinking behavior

Baseline behavior and behavior only cohort with a thirst stimulus was measured using the Coulbourn Habitest system® (Harvard Apparatus). For food consumption behavior, regular pellets (BioServ Dustless Precision Pellets, F0071) were dispensed from an automatic feeder operated by an optical sensor. The weight of individual pellet was measured by weighing 50 pellets 5 times independently, and was 18.0 mg (mean) +/- 0.3 mg (standard deviation). For water consumption behavior, contact lickometers were manually built to detect and record individual licks[4]. To measure the volume of individual water licks, the water bottle was weighed at the beginning and the end of an overnight session of ad libitum feeding and drinking in the behavioral chamber, and the volume of consumed water was divided by the total number of licks, yielding 1.21 µL (mean) +/- 0.02 µL (standard deviation). For baseline behavior, mice were given *ad libitum* access to pellets and water to measure

bioRxiv preprint doi: https://doi.org/10.1101/2024.09.26.615271; this version posted September 27, 2024. The copyright holder for this preprint (which was not certified by peer review) is the author/funder, who has granted bioRxiv a license to display the preprint in perpetuity. It is made available under aCC-BY-NC-ND 4.0 International license.

baseline food and water intake behavior for 24 hours. For prandial thirst behavior, mice were fasted overnight with access to water and given ad libitum access to pellets for 30 minutes with the water spout blocked. After 30 minutes, the pellet dispenser was stopped and the water spout was exposed for water lick measurement for the following 30 minutes. For baseline behavior and prandial thirst behavior, crumbs generated during pellet consumption were collected on a tray underneath the behavioral chamber and were weighed after the experiment for subsequent correction of total food intake. For water deprivation thirst behavior, mice were water deprived for 24 hours in their home cage with access to chow prior to the water lick measurement in the behavior chamber. For osmotic thirst behavior, mice were intraperitoneally injected with 2 M NaCl. For hypovolemic thirst behavior, mice were subcutaneously injected with 40% of polyethylene glycol in their shoulder. All mice were habituated to the behavioral chamber, lickometer and/or feeder one overnight prior to the experiments. All behavioral recordings started after mice were initially acclimated to the behavioral chamber for 15 minutes. Mice had at least 24 hours of recovery after each experiment before initiation of a different thirst paradigm.

Behavioral analysis

Behavioral data was collected by Graphic State software and subsequently analyzed using custom-written python scripts. Water lick bouts were defined as 10 or more water licks spaced by 1 second or less[5].

Lever press operant task

A lever-press operant task was conducted using a Coulbourn Habitest system® (Harvard Apparatus). A water spout was connected to a solenoid valve (LEE company #LHLA2431111H) via a custom-designed circuit. Pressing the designated active lever (but not the inactive lever) triggered the valve to open for 50 milliseconds, delivering a water reward of about 6.49 µL. Three reinforcement schedules were employed: In Fixed Ratio 1 (FR1), a single press on the active lever resulted in one valve opening event and water delivery. In Fixed Ratio 5 (FR5), five consecutive presses on the active lever were required for a single valve opening event and water delivery. In Progressive Ratio (PR), the number of active lever presses needed for a valve opening event and water delivery progressively increased in a fixed-increment sequence (in multiples of 3: 3, 6, 9, 12, ...).

Mice were initially trained for the task using the FR1 schedule for five consecutive nights before FR1 experiments. Following FR1 experiments, mice underwent training on the FR5 schedule for three nights prior to FR5 experiments. Finally, the PR schedule was implemented. Overnight training was performed with ad libitum access to chow. For all lever press experiments, mice were water deprived for 24 hours

bioRxiv preprint doi: https://doi.org/10.1101/2024.09.26.615271; this version posted September 27, 2024. The copyright holder for this preprint (which was not certified by peer review) is the author/funder, who has granted bioRxiv a license to display the preprint in perpetuity. It is made available under aCC-BY-NC-ND 4.0 International license.

prior to the experiment. Following water deprivation, mice were acclimated to the behavioral chamber for 15 minutes. During acclimation, the wall containing the levers and water spout remained occluded to prevent interaction with the operant conditioning apparatus After 15 minutes, experiments started with the levers and water spout exposed. Mean number of lever press was plotted by aligning to the first lever press.

Stereotaxic surgery

For PVH-AVP fiber photometry recordings, AVP-Cre/+ mice were injected with 150 nL of AAV1.CAG.flex.GCaMP6s (Janelia Vector Core, $4.73x10^{13}$ vg/mL) into the PVH (−0.7 mm AP, +0.3 mm ML, −4.7 mm DV). In the same surgery, an optical fiber (Doric Lenses, 0.4 mm inner diameter and 5.4−6.0 mm length, MFC_400/430-0.48) was implanted in the same coordinate as the injection site.

For SFO-Glut fiber photometry recordings, wild-type mice were injected with 200 nL of AAV9.CaMKII.GCaMP6s.WPRE (Janelia Vector Core, $2.17x10^{14}$ vg/mL) freshly diluted 1/10 with sterile PBS into the SFO (-0.65 mm AP, 0 mm ML, −2.7 mm DV). In the same surgery, an optical fiber (Doric Lenses, 0.4 mm inner diameter and 3.0−3.5 mm length, MFC_400/430-0.48) was implanted at -0.65 mm AP, 0 mm ML, −2.85 mm DV in young animals and −0.65 mm AP, 0 mm ML, −2.9 mm DV in aged animals.

For NAc-DA fiber photometry recordings, wild-type mice were injected with 200 nL of AAV9.hSyn.GRAB-DA3m (WZ Biosciences, $5.80x10^{13}$ vg/mL) into the NAc shell (+1.0 mm AP, +1.4 mm ML, −4.5 mm DV). In the same surgery, an optical fiber (Doric Lenses, 0.4 mm inner diameter and 5.0−5.4 mm length, MFC_400/430-0.48) was implanted in the same coordinate as the injection site.

For SFO optogenetics experiments, wild-type mice were injected with 150 nL of AAV5.CaMKIIa.hChR2 (Janelia Vector Core, $7.36x10^{12}$ vg/mL) into the SFO (−0.65 mm AP, 0 mm ML, −2.65 mm DV). In the same surgery, an optical fiber (Thorlabs, 200 μm) was manually trimmed and polished to 3.0−3.5 mm length and implanted 0.25 mm above the injection site.

Following surgical implantation, all mice were allowed a recovery period of two weeks and were habituated in the behavioral chamber overnight with a lickometer prior to fiber photometry or optogenetic experiments.

Fiber photometry recording and analysis

Tethering and light delivery: Implanted mice were secured with a patch cable (Doric Lenses, MFP_400/460/900-0.48_2m_FCM-MF2.5). Continuous excitation light was provided by two light-emitting diodes (LEDs): a 6 mW blue LED with a wavelength of 470 nm and a UV LED with a

bioRxiv preprint doi: https://doi.org/10.1101/2024.09.26.615271; this version posted September 27, 2024. The copyright holder for this preprint (which was not certified by peer review) is the author/funder, who has granted bioRxiv a license to display the preprint in perpetuity. It is made available under aCC-BY-NC-ND 4.0 International license.

wavelength of 405 nm. A multichannel hub from Thorlabs served as the power source for the LEDs. To differentiate between signals, these LEDs were modulated at distinct frequencies of 211 Hz and 511 Hz, respectively. A filtered minicube (Doric Lenses, FMC6_AE(400-410)_E1(450-490)_F1(500-540)_E2(550-580)_F2(600-680)_S) ensured that only specific wavelengths reached the implant. The filtered light was then channeled via optical fibers (Doric Lenses, MFC_400/430-0.48) to the implanted device.

Signal acquisition and processing: Light signals originating from either GCaMP or GRAB-DA, along with UV isosbestic point signals, were simultaneously collected through the same optical fibers using a femto-watt silicon photoreceiver (Newport, 2151). The collected digital signals were amplified using a lock-in amplifier to enhance the desired signal and eliminate background noise. Then, they were demodulated using their corresponding modulation frequencies (211 Hz and 511 Hz) to separate the signals originating from the two LEDs. Finally, an RZ5P processor (Tucker-Davis Technologies) processed the signals for further analysis. The processed data from the fiber photometry recordings were collected and stored using Synapse software (TDT).

Lickometer recording and data analysis: A custom-designed lickometer based on the work of Slotnick (2009) was employed to detect individual water lick events. These lick events were time-stamped and recorded by the TDT software throughout the fiber photometry recording session. After data exportation via Browser (TDT), custom Python scripts were used to analyze the data following downsampling at a rate of 1/125.

Data processing: GCaMP or GRAB-DA signals were normalized by UV signals, and z score was used for plots and subsequent analysis ($z = (x-\mu)/\sigma$, z is the raw signal, μ is the population mean, and σ is the population standard deviation). z score values were smoothened by a factor of 101 using the Hanning window for calculating half time for GCaMP activation and linear regression fitting during SFO-Glut GCaMP inactivation.

Recording of feeding behavior: For prandial thirst, animals were fasted overnight and given access to standard chow (PicoLab Rodent Diet 20, 5053) without water for the first 30 minutes, followed by chow removal and water access for the next 30 minutes. Chow was weighed before and after the experiment and fallen chow crumbs were weighed to obtain true chow consumption. Chow intake was video recorded with an infra-red camera and iSpy software. Individual chow bite events were scored using the

bioRxiv preprint doi: https://doi.org/10.1101/2024.09.26.615271; this version posted September 27, 2024. The copyright holder for this preprint (which was not certified by peer review) is the author/funder, who has granted bioRxiv a license to display the preprint in perpetuity. It is made available under aCC-BY-NC-ND 4.0 International license.

BORIS software[6]. To note, standard chow was provided on the floor of the chamber instead of utilizing the automated pellet dispenser. This modification was necessary due to physical incompatibility between the fiber optic implants on the mouse head and the design of the feeding trough associated with the automated pellet dispenser.

Reagent preparation: 2 M NaCl was prepared in water and intraperitoneally injected at 250 µL/35 g body weight. 40% polyethylene glycol (PEG 400, Sigma #807485) was prepared in water and subcutaneously injected in the shoulder at 300 µL/20 g body weight. Angiotensin II (AngII, Anaspec, AS-20633) stock was prepared in PBS (10 µg/µL), kept in -80°C in aliquots, and prepared fresh on the day of experiment for subcutaneous injection at 3.0 mg/kg body weight in PBS. Histamine (Millipore Sigma, #59964) stock was prepared in PBS (100 mg/1.5 mL), kept in -20°C in aliquots, and prepared fresh on the day of experiment for subcutaneous injection at 5.0 mg/kg body weight in PBS.

Optogenetic stimulation

For optogenetic stimulation of SFO-Glut neurons, mice were either well-hydrated or water deprived for 24 hours in their home cages, acclimated to the behavioral chamber for 15 minutes, then provided access to water for 15 min with or without optical stimulation (15 mW, 20 Hz) using a DPSS 532 nm laser (Shanghai Laser and Optics Century). Water lick events were recorded for 30 minutes. For terminal SFO-Glut stimulation for c-fos immunohistochemistry, mice were photo-stimulated for 15 minutes (15 mW, 20 Hz), waited for 90-120 minutes, then transcardiac perfused with saline followed by 4% paraformaldehyde for collection of the brain.

Immunohistochemistry

At the end of their experiments, mice were transcardiac perfused with saline followed by 4% paraformaldehyde (PFA). Brain was collected and incubated in 4% PFA overnight at 4°C, followed by incubation in 30% sucrose in PBS at 4°C for 1-3 days, freezing in the OCT cryoprotectant compound (Tissue-Tek) and storage at -80°C. Frozen brains were sectioned in 30-40 µm thickness and incubated in normal goat serum (NGS) for 1 hour in RT, stained with primary antibodies for one overnight at 4°C, washed in 10% Triton-X in PBS three times, stained with secondary antibodies for 1 hour in RT, and washed in PBS three times before mounting onto the glass slide for microscopy. Brain sections were imaged using Zeiss LSM 700 confocal microscope and Nikon Eclipse Ti2 microscope. For GCaMP and GRAB-DA, chicken anti-GFP polyclonal antibody (Abcam, ab13970, 1:2000) and goat anti-chicken IgY (H+L) antibody, Alexa Fluor™ 488 (Thermo Fisher, A-11039, 1:1000) was used primary and secondary staining, respectively. For AVP, rabbit anti-AVP polyclonal antibody (Sigma-Aldrich, AB1565, 1:1000)

bioRxiv preprint doi: https://doi.org/10.1101/2024.09.26.615271; this version posted September 27, 2024. The copyright holder for this preprint (which was not certified by peer review) is the author/funder, who has granted bioRxiv a license to display the preprint in perpetuity. It is made available under aCC-BY-NC-ND 4.0 International license.

and goat anti-rabbit IgG (H&L) antibody, Alexa Fluor® 568 (abcam, ab175471, 1:1000) was used for primary and secondary staining, respectively.

Statistics and figures

Statistical analyses were performed using the Prism software. Schematics for experimental procedures were generated using Biorender.

References for Methods

1. Richter, C. P. & Brailey, M. E. WATER-INTAKE AND ITS RELATION TO THE SURFACE AREA OF THE BODY. *Proc. Natl. Acad. Sci. U.S.A.* **15**, 570–578 (1929).

2. Tordoff, M. G., Bachmanov, A. A. & Reed, D. R. Forty mouse strain survey of water and sodium intake. *Physiology & Behavior* **91**, 620–631 (2007).

3. Wegner, K. A. *et al.* Void spot assay procedural optimization and software for rapid and objective quantification of rodent voiding function, including overlapping urine spots. *American Journal of Physiology-Renal Physiology* **315**, F1067–F1080 (2018).

4. Slotnick, B. A SIMPLE 2-TRANSISTOR TOUCH OR LICK DETECTOR CIRCUIT. *J Exper Analysis Behavior* **91**, 253–255 (2009).

5. Zimmerman, C. A. *et al.* Thirst neurons anticipate the homeostatic consequences of eating and drinking. *Nature* **537**, 680–684 (2016).

6. Friard, O. & Gamba, M. BORIS : a free, versatile open-source event-logging software for video/audio coding and live observations. *Methods Ecol Evol* **7**, 1325–1330 (2016).

Author contributions

H.J., Z.A.K. and J.L.G. conceived the project and designed experiments. H.J. led and performed experiments. H.J, Z.A.K. and J.L.G. analysed and interpreted data. H.J., A.B.S., U.D. and J.H.W. collected plasma and urine samples and measured the parameters. H.J., A.B.S. and U.D. performed behavioral experiments. H.J., A.B.S. and J.H.W. performed the photometry experiments. H.J. and A.B.S. performed the optogenetic experiments. H.J. performed all the photometry and optogenetic surgeries. H.J., A.B.S. and J.H.W. performed histology. H.J, Z.A.K. and J.L.G wrote the manuscript.

bioRxiv preprint doi: https://doi.org/10.1101/2024.09.26.615271; this version posted September 27, 2024. The copyright holder for this preprint (which was not certified by peer review) is the author/funder, who has granted bioRxiv a license to display the preprint in perpetuity. It is made available under aCC-BY-NC-ND 4.0 International license.

Acknowledgements

We thank members of the Garrison and Knight labs for constructive discussions; Sarah Shehata for assistance with analyzing chow feeding videos; and Cyrus Ghiassi, Alba Villagrana and Elizabeth Poznyakov for assistance with imaging void spot papers. This work was funded in part by the NIH (R35 GM119828 and R35 GM145305 to J.L.G., T32AG000266 and F32AG063488 to H.J.), and the Glenn Foundation for Medical Research (to H.J.). Zachary A. Knight is a Howard Hughes Investigator.

bioRxiv preprint doi: https://doi.org/10.1101/2024.09.26.615271; this version posted September 27, 2024. The copyright holder for this preprint (which was not certified by peer review) is the author/funder, who has granted bioRxiv a license to display the preprint in perpetuity. It is made available under aCC-BY-NC-ND 4.0 International license.

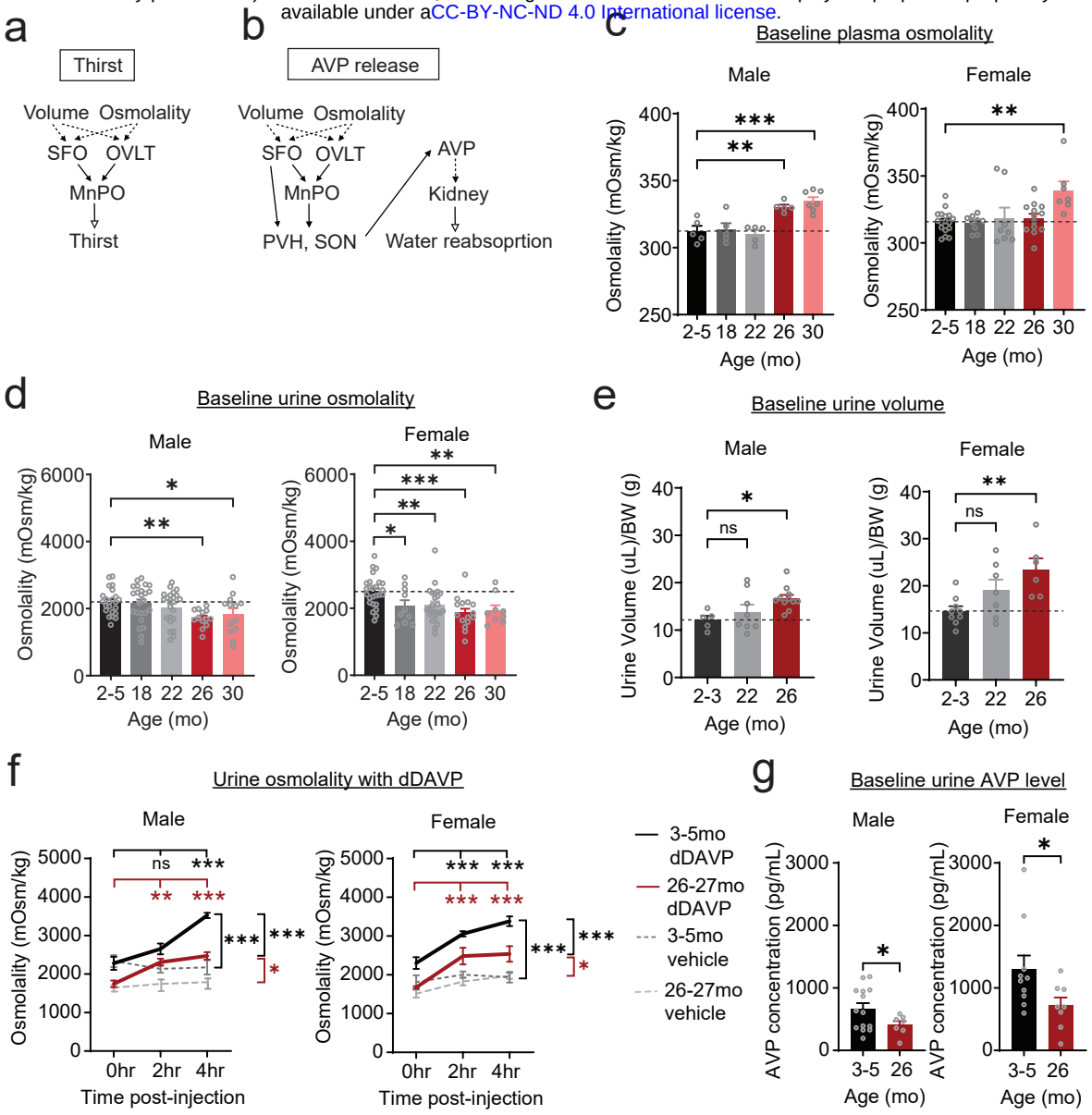

Figure 1. Aged mice are chronically dehydrated and have renal dysfunction.

a. A schematic of the neural pathway for thirst. Volume and osmolality changes are sensed by Subfornical Organ (SFO) and Organum Vasculosum of the Lamina Terminalis (OVLT) and the signals are relayed to their downstream nuclei, median preoptic nucleus (MnPO). **b.** A schematic of the neural pathway for AVP release. Volume and osmolality changes are sensed by SFO and the signals are relayed to the downstream nuclei, MnPO. Both SFO and MnPO project to the paraventricular (PVH) and supraoptic (SON) hypothalamus where AVP is released into circulation and promotes water reabsorption in the kidney. **a,b.** Closed arrows with solid lines represent neural innervations; closed arrows with dotted lines, sensing of circulatory signals; open arrows with solid lines, functional outcomes **c.** Plasma osmolality in 2-5, 18-19, 22-23, 26-27 and 30-31 month-old male and female mice in their baseline state with free access to chow and water. Male, ***P<0.001 and female, **P<0.01 by one-way ANOVA.**P<0.01 and ***P<0.001 by Fisher's LSD test. **d.** Urine osmolality in 2-5, 18-19, 22-23, 26-27 and 30-31 month-old male and female mice in their baseline state with free access to chow and water. Male, *P<0.05 and female, ***P<0.001 by one-way ANOVA. *P<0.05, **P<0.01 and ***P<0.001 by Fisher's LSD test. **e.** Urine volume for 4 hours in 2-3, 22-23 and 26-27 month-old male and female mice adjusted by body weight in 2-3, 22-23 and 26-27 months old male and female mice. Male, *P<0.05 and female, **P<0.01 by one-way ANOVA. ns, non-significant; *P<0.05, **P<0.01 by Dunnet's test. **f.** Urine osmolality in 3-5 and 26-27 month-old male and female mice before and after dDAVP (1 mg/kg BW) or vehicle injection. For males, ***P<0.001 for main effects of dDAVP [F(2, 80)=14.78] and age [F(3, 80)=34.57], and ***P<0.001 for interactions of their main effects [F(6, 80)=7.240] by 2-way ANOVA. For females, ***P<0.001 for main effects of dDAVP [F(2, 64)=23.50] and age [F(3, 64)=49.55], and *P<0.05 for interactions of their main effects [F(6, 64)=2.775] by 2-way ANOVA. ns, non-significant; *P<0.05 and ***P<0.001 compared to the baseline value or by Dunnet's test. Values at 4 hours post-dDAVP and post-vehicle within the age group were compared (*P<0.05 and ***P<0.001 by Sidak's test). Values at 4 hours post-dDAVP were compared between age groups (male, ***P<0.001 and female, ***P<0.001 by Sidak's test). **g.** Urine AVP levels in 3-5 and 26-27 months-old male and female mice in the baseline state. *P<0.05 by student's t-test.

bioRxiv preprint doi: https://doi.org/10.1101/2024.09.26.615271; this version posted September 27, 2024. The copyright holder for this preprint (which was not certified by peer review) is the author/funder, who has granted bioRxiv a license to display the preprint in perpetuity. It is made available under aCC-BY-NC-ND 4.0 International license.

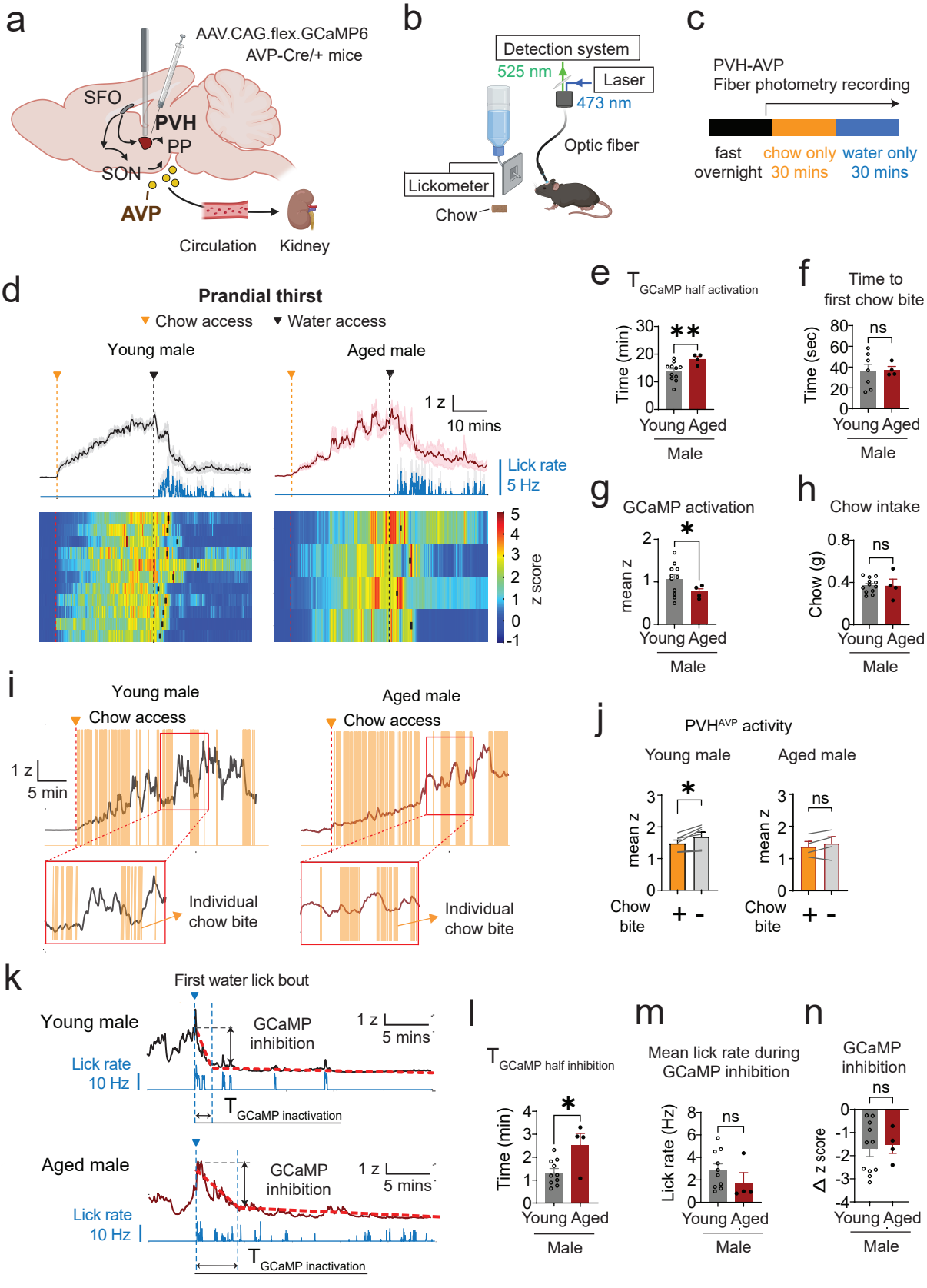

bioRxiv preprint doi: https://doi.org/10.1101/2024.09.26.615271; this version posted September 27, 2024. The copyright holder for this preprint (which was not certified by peer review) is the author/funder, who has granted bioRxiv a license to display the preprint in perpetuity. It is made available under aCC-BY-NC-ND 4.0 International license.

Figure 2. Age delays PVH^{AVP} neuronal responses to feeding and drinking.

a. Schematic for the stereotaxic injection of AAVs cre-dependently expressing GCaMP in the PVH and implant of optic fiber for fiber photometry. AVP, Arginine Vasopressin. PVH, Paraventricular Nucleus of the Hypothalamus, PP, Posterior Pituitary. SON, Supraoptic Nucleus. SFO, Subfornical Organ. Arrows represent synaptic projections.
b. Schematic for PVH^{AVP} fiber photometry recording during dry chow intake and subsequent water drinking.
c. Fiber photometry recording paradigm during 30 minute chow intake after overnight fasting followed by 30 minutes of water intake.
d. (Top) Mean lick rate (blue) and mean z-score trace of GCaMP fluorescence in young (3-4 mo, black solid) and aged (24-26 mo, magenta solid) male mice, aligned by chow access (red dotted vertical line). (Bottom) Heatmap of individual z-score traces in each group. Black dotted lines represent water access. A black rectangle represents the beginning of water lick bout in each recording.
e. Time for GCaMP to rise from the baseline to the half peak z-score of GCaMP fluorescence. **P<0.01 by Welch's t-test.
f. Latency from the chow access to the first chow bite in each animal. ns., non-significant.
g. Mean z-score of GCaMP fluorescence from chow access (t=0, red dotted vertical line in d) to water access (t=30 mins, black dotted vertical line in d). *P<0.05 by Welch's t-test.
h. Amount of chow intake during 30 minutes of chow access. ns., non-significant.
i. Individual z-score traces of GCaMP fluorescence from PVH^{AVP} fiber photometry recording during feeding chow without water after overnight fasting. Dotted red lines represent chow access. Yellow solid vertical bars represent individual chow bite events. Example traces are from (left) 4- and (right) 26- month-old male mice. Red boxes show zoomed in GCaMP trace and individual chow bite events.
j. Mean z score during chow bite (on chow) and between chow bites (off chow) in young and aged male mice. ***P<0.001 and *P<0.05 for main effects of chow bite [F(1, 18)=28.81] and age [F(1, 18)=5.316], respectively, and **P<0.01 for interactions of their main effects [F(1, 18)=8.899] by 2-way ANOVA. ns., non-significant and ***P<0.001 by Sidak's test.
k. Example traces of lick rate (blue) and mean z-score trace of GCaMP fluorescence in (top) 4-month-old male (black solid) and (bottom) 26-month-old male (magenta solid) mice, aligned by the first water lick bout. Red dotted lines represent fitted linear regression lines for the fast PVH^{AVP} inhibition phase and the steady phase.
l. Half time for GCaMP to reach the transition point from the fast PVH^{AVP} inhibition phase to the steady phase as indicated in **k.** *P<0.05 by unpaired t-test.
m. Mean lick rate during the fast PVH^{AVP} inhibition phase. ns, non-significant by unpaired t-test.
n. Magnitude of PVH^{AVP} inhibition during the fast inhibition phase as indicated in **k.** ns. non-significant and ns, non-significant by unpaired t-test.

bioRxiv preprint doi: https://doi.org/10.1101/2024.09.26.615271; this version posted September 27, 2024. The copyright holder for this preprint (which was not certified by peer review) is the author/funder, who has granted bioRxiv a license to display the preprint in perpetuity. It is made available under aCC-BY-NC-ND 4.0 International license.

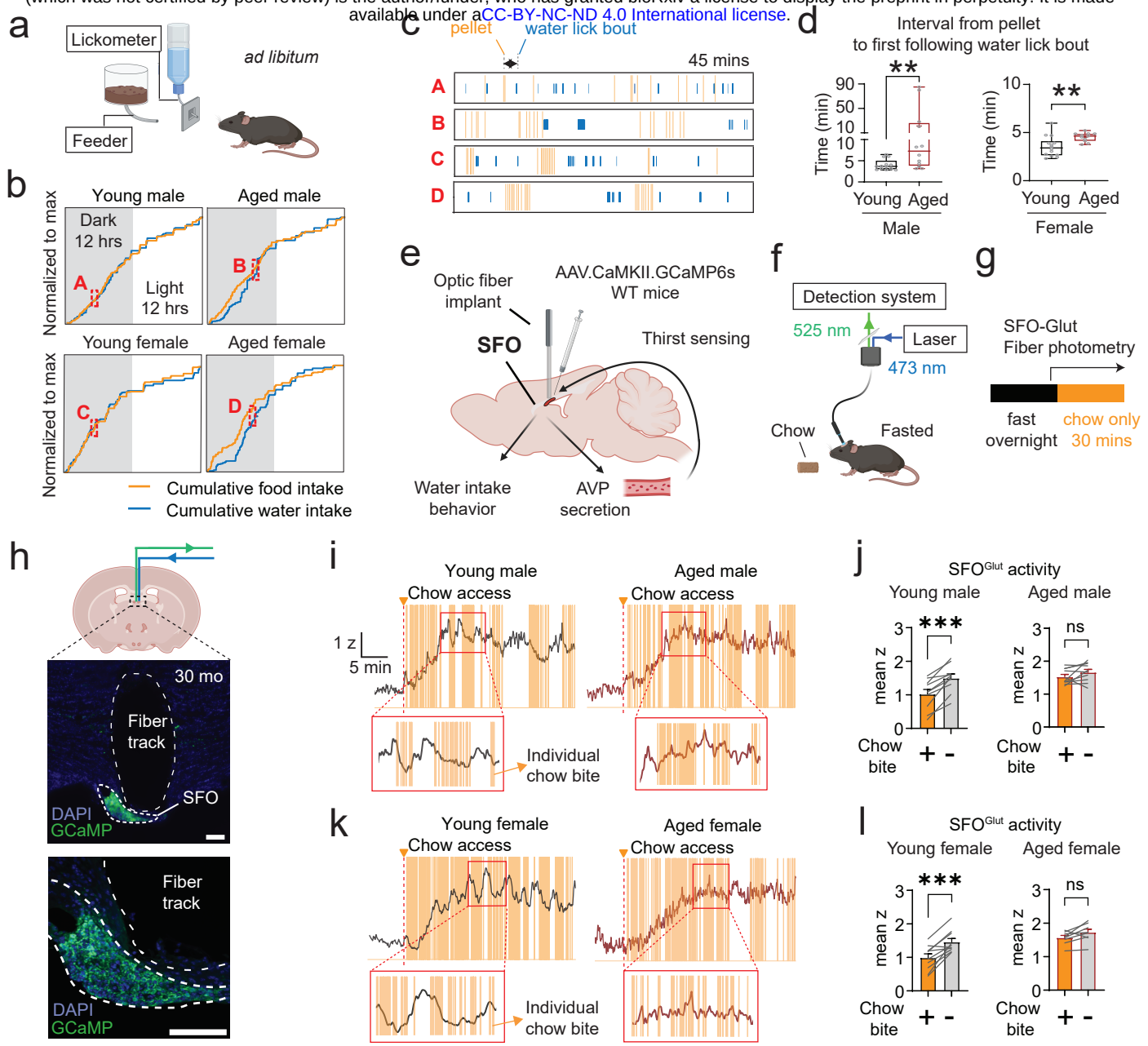

Figure 3. Age delays feeding-induced water drinking

a. Schematic for *ad libitum* food and water intake behavior. **b.** Individual examples of cumulative food and water intake over 24 hours, normalized by total food and water intake, respectively, from 3 month-old male and female mice and 27 months-old male and female mice. First 12 hours are during the dark cycle (gray shaded area), followed by 12 hours of light cycle. **c.** 45 minutes of zoomed-in raster plots from gray and red dotted boxes from **2e**. Brown bars represent individual pellet intake and blue bars represent individual water lick events. **d.** Box-whisker plot of time interval from each pellet intake to the first following water lick bout. Each dot represents a median value during 24 hours from an individual mouse in each sex/age group. **P<0.01 by Mann-Whitney test. Scheme for fiber photometry recording of the SFOGlut neuronal activity during chow intake and prandial drinking behavior. **e.** Schematic for the stereotaxic injection of AAVs expressing GCaMP in the SFO and implant of optic fiber for fiber photometry. SFO senses thirst signals in circulation and modulates water intake and AVP secretion. **f.** Schematic for SFO^{Glut} fiber photometry recording during dry chow intake. **g.** Experimental paradigm for SFO^{Glut} fiber photometry recording during 30 minute chow intake after overnight fasting.**h.** (Top) Coronal section of the mouse brain with SFO in the dotted box for fiber photometry. (Middle) GCaMP expression (in green) in the SFO and fiber track (dotted outline) of a 30 months old male mouse. Scale bar represents 100 µm. (Bottom) Zoomed-in image of GCaMP expression in the SFO and fiber track. Scale bar represents 100 µm. **i.** Individual z-score traces of GCaMP fluorescence from SFO fiber photometry recording during feeding chow without water after overnight fasting. Dotted red lines represent chow access. Yellow solid vertical bars represent individual chow bite events. Example traces are from (left) 3- and (right) 26- month-old male mice. Red boxes show zoomed in GCaMP trace and individual chow bite events. **j.** Mean z score during chow bite and between chow bites in young and aged male mice. ns, non-significant and ***P<0.001 by paired t-test. **k.** Individual z-score traces of GCaMP fluorescence from SFO^{Glut} fiber photometry recording during feeding chow without water after overnight fasting. Dotted red lines represent chow access. Yellow solid vertical bars represent individual chow bite events. Example traces are from (left) 4- and (right) 27- month-old female mice. Red boxes show zoomed in GCaMP trace and individual chow bite events.

bioRxiv preprint doi: https://doi.org/10.1101/2024.09.26.615271; this version posted September 27, 2024. The copyright holder for this preprint (which was not certified by peer review) is the author/funder, who has granted bioRxiv a license to display the preprint in perpetuity. It is made available under aCC-BY-NC-ND 4.0 International license.

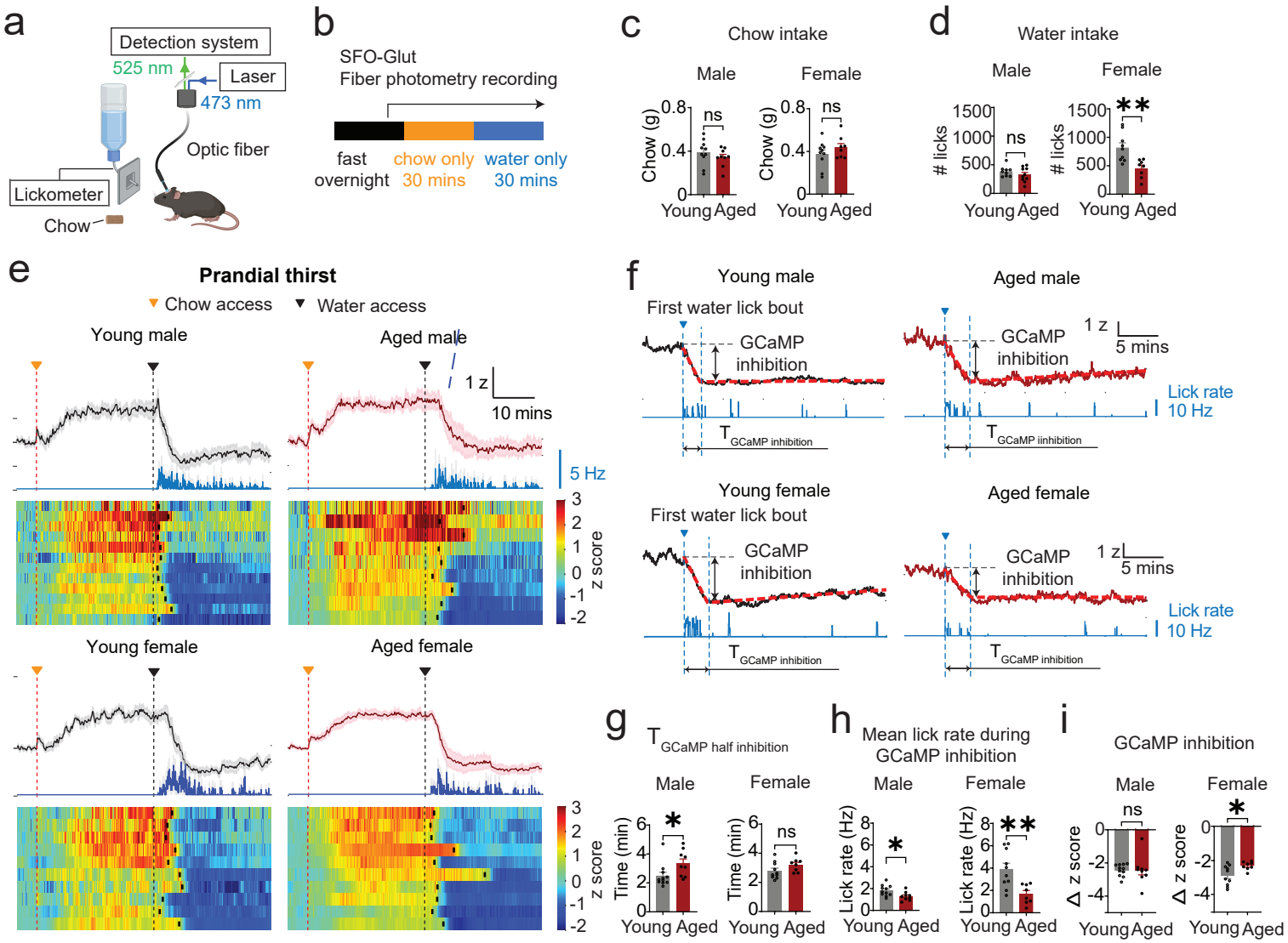

Figure 4. Age reduces water intake after feeding in females and delays SFO^{Glut} neuronal inhibition by rehydration.

a. Behavioral setup for SFO^{Glut} fiber photometry recording during dry chow intake and prandial drinking behavior. **b.** Experimental paradigm for SFO^{Glut} fiber photometry recording during 30 minute chow intake after overnight fasting followed by 30 minutes of water intake. **c.** Amount of chow intake during 30 minutes of chow access. n.s., non-significant by unpaired t-test. **d.** Number of total water licks during 25 minutes following 30 minutes of chow intake. n.s., non-significant and **P<0.01 by unpaired t-test. **e.** (Top) Mean lick rate (blue) and mean z-score trace of GCaMP fluorescence in young (2-5 mo, black solid) and aged (25-27 mo, magenta solid) male and female mice, aligned by chow access (red dotted vertical line). (Bottom) Heatmap of individual z-score traces in each group. Black dotted lines represent water access. A black rectangle represents the beginning of water lick bout in each recording. **f.** Examples of lick rate (blue) and z-score trace of GCaMP fluorescence during water drinking after feeding, aligned by the first water lick bout (blue dotted line with a blue triangle). (Top left) 3- and (top right) 26- month-old male mice and (bottom left) 4- and (bottom right) 27- month-old female mice. Red dotted lines represent fitted linear regression lines for the fast SFO inhibition phase and the steady phase. **g.** Half time for GCaMP to reach the transition point from the fast SFO inhibition phase to the steady phase. n.s., non-significant and *P<0.05 by unpaired t-test. **h.** Mean lick rate during the fast SFO inhibition phase. *P<0.05 and **P<0.01 by unpaired t-test. **i.** Magnitude of SFO^{Glut} inhibition during the fast SFO^{Glut} inhibition phase as indicated in **f.** ns. non-significant and *P<0.05 by unpaired t-test.

bioRxiv preprint doi: https://doi.org/10.1101/2024.09.26.615271; this version posted September 27, 2024. The copyright holder for this preprint (which was not certified by peer review) is the author/funder, who has granted bioRxiv a license to display the preprint in perpetuity. It is made available under aCC-BY-NC-ND 4.0 International license.

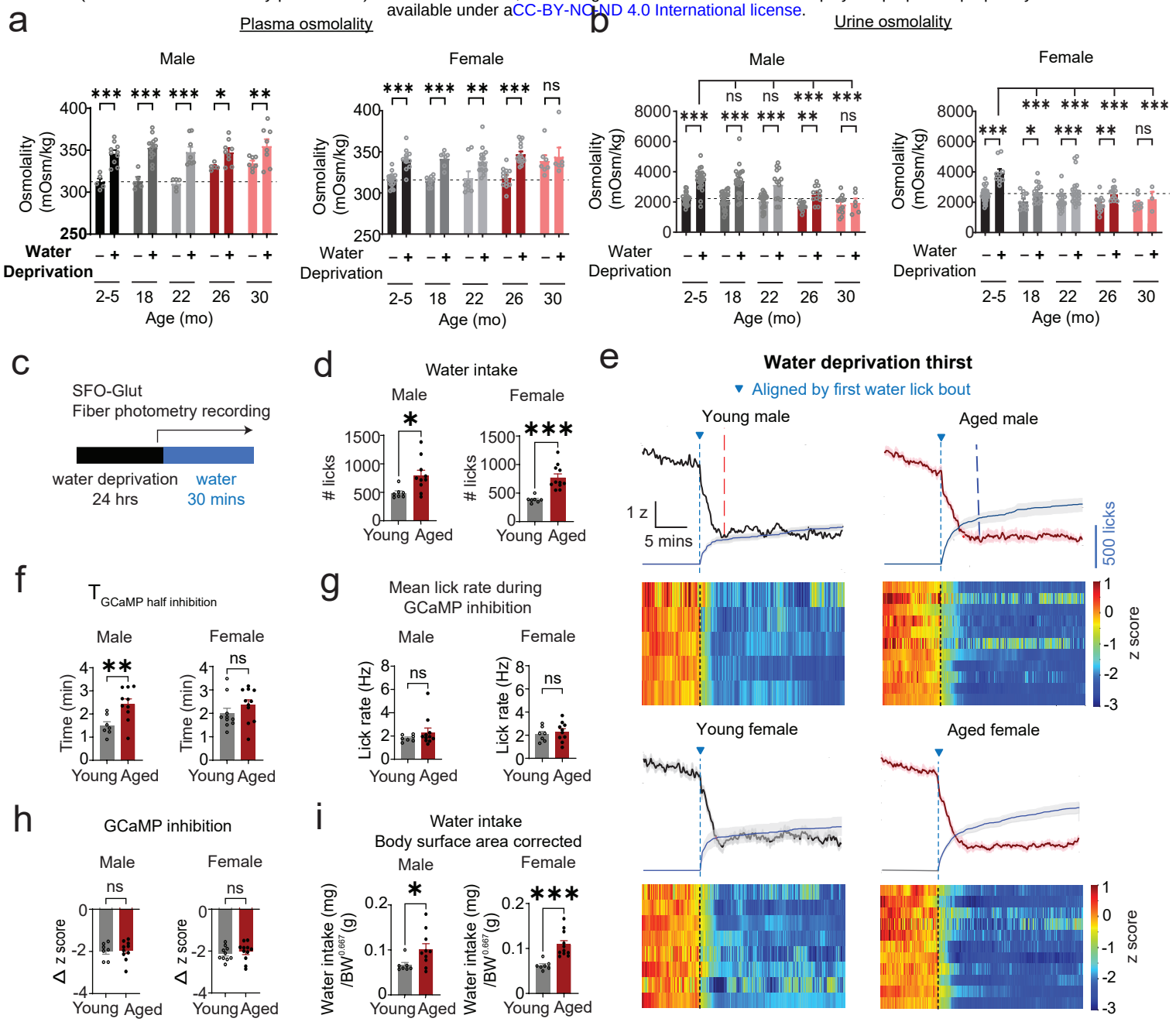

Figure 5. Age increases water intake after deprivation and delays SFO^{Glut} neuronal inhibition by rehydration. **a.** Plasma osmolality during baseline with free access to food and water and after 24 hours of water deprivation in young (2-5 mo) and aged (26-27 mo) male (left) and female (right) mice. ns, non-significant, *P<0.05, **P<0.01 and ***P<0.001 by Fisher's LSD test. For males, ***P<0.001 and *P<0.05 for main effects of hydration state [F(4, 66)=1.886] and age [F(1, 66)=79.26] respectively, and non-significant for interactions of their main effects [F(4, 66)=3.403] by 2-way ANOVA. For females, ***P<0.001 and *P<0.05 for main effects of hydration state [F(1, 99)=53.33] and age [F(4, 99)=2.493] respectively, and non-significant for interactions of their main effects [F(4, 99)=1.715] by 2-way ANOVA. **b.** Urine osmolality during baseline with free access to food and water and after 24 hours of water deprivation in young (2-5 mo) and aged (26-27 mo) male (left) and female (right) mice. ns, non-significant, *P<0.05, **P<0.01 and ***P<0.001 by Fisher's LSD test. For males, ***P<0.001 for main effects of hydration state [F(4, 161)=69.12] and age [F(4, 161)=10.85], and *P<0.05 for interactions of their main effects [F(4, 161)=3.056] by 2-way ANOVA. For females, ***P<0.001 for main effects of hydration state [F(1, 135)=37.47] and age [F(4, 135)=12.88], and *P<0.05 for interactions of their main effects [F(4, 135)=2.670] by 2-way ANOVA. **c.** Behavioral paradigm of SFO^{Glut} fiber photometry recording during 30 minutes of water intake after 24 hours of water deprivation. **d.** Number of total water licks during 25 minutes. *P<0.05 and ***P<0.001 by unpaired t-test. **e.** (Top) Mean cumulative number of licks (blue) and mean z-score trace of GCaMP fluorescence in young (3-6 mo, black solid) and aged (26-28 mo, magenta solid) male and female mice, aligned by first water lick bout (blue dotted vertical line). (Bottom) Heatmap of individual z-score traces in each group. **f.** Half time for GCaMP to reach the transition point from the fast SFO^{Glut} inhibition phase to the steady phase. n.s., non-significant and **P<0.01 by unpaired t-test. **g.** Mean lick rate during the fast SFO^{Glut} inhibition phase. n.s., non-significant by unpaired t-test. **h.** Magnitude of SFO^{Glut} inhibition during the fast SFO^{Glut} inhibition phase as indicated in e. n.s., non-significant by unpaired t-test.

bioRxiv preprint doi: https://doi.org/10.1101/2024.09.26.615271; this version posted September 27, 2024. The copyright holder for this preprint (which was not certified by peer review) is the author/funder, who has granted bioRxiv a license to display the preprint in perpetuity. It is made available under aCC-BY-NC-ND 4.0 International license.

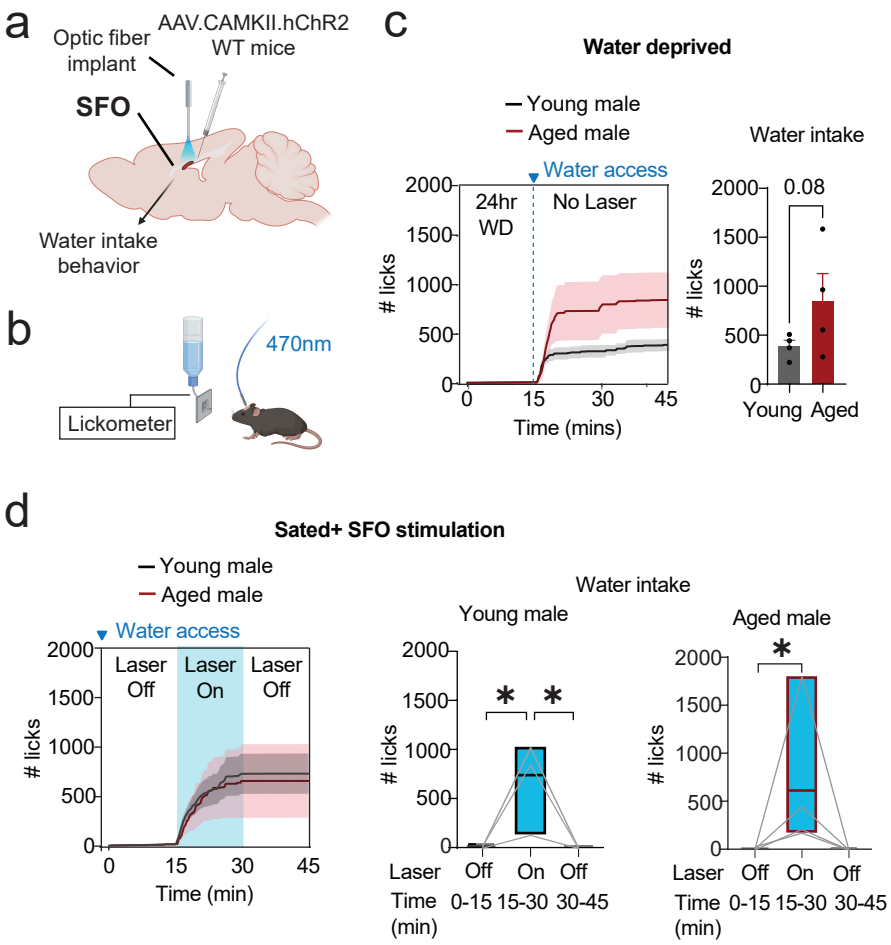

Figure 6. Age preserves the SFO^{Glut} synaptic output for water intake behavior.

a. Schematic for the stereotaxic injection of AAV driving ChR2 in the SFO and implant of optic fiber for optogenetic laser stimulation. **b.** Schematic for optogenetic stimulation and recording of water intake behavior. **c.** (Left) Cumulative number of licks in mice that were water deprived for 24 hours. Water access was given between 15-45 minutes of behavioral recording and no laser light was delivered. Total number of licks in young (middle) and aged (right) male mice for 30 minutes after water access. P = 0.08 by ratio paired t-test. **d.** (Left) Cumulative number of licks in mice that were satiated and well hydrated. 470 nm laser light was delivered at 20 Hz between 15-30 minutes only (blue shaded area). Total number of licks in young (middle) and aged (right) male mice during 0-15 minutes (laser off), 15-30 minutes (laser on) and 30-45 minutes (laser off). *P<0.05 by ratio paired t-test.

bioRxiv preprint doi: https://doi.org/10.1101/2024.09.26.615271; this version posted September 27, 2024. The copyright holder for this preprint (which was not certified by peer review) is the author/funder, who has granted bioRxiv a license to display the preprint in perpetuity. It is made available under aCC-BY-NC-ND 4.0 International license.

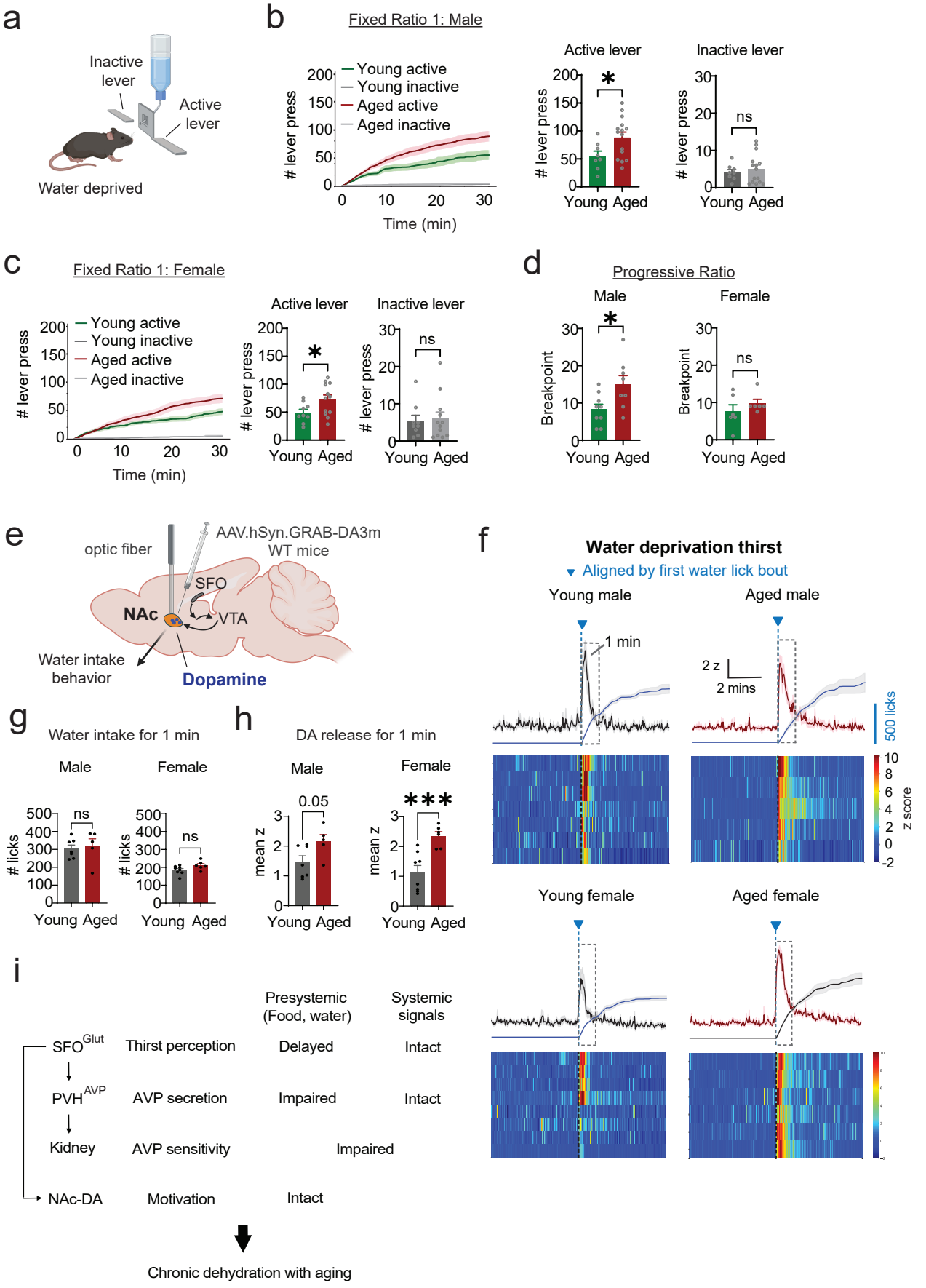

bioRxiv preprint doi: https://doi.org/10.1101/2024.09.26.615271; this version posted September 27, 2024. The copyright holder for this preprint (which was not certified by peer review) is the author/funder, who has granted bioRxiv a license to display the preprint in perpetuity. It is made available under aCC-BY-NC-ND 4.0 International license.

Figure 7. Age increases motivation for water after deprivation.
a. Schematic for lever press operant task for water after 24 hours of water deprivation.
b. Fixed Ratio 1 (FR1) in operant task for water for 30 minutes in water deprived young (2-5 mo, green line) and aged (23-28 mo, magenta line) mice. (Left) Cumulative number of lever presses over time. (Middle) Total number of active lever presses in 30 minutes. (Right) Total number of inactive lever presses in 30 minutes. ns, non-significant and *P< 0.05 by unpaired t-test.
c. Fixed Ratio 1 (FR1) in operant task for water for 30 minutes in water deprived young (2-6 mo, green line) and aged (23-27 mo, magenta line) female mice. (Left) Cumulative number of lever presses over time. (Middle) Total number of active lever presses in 30 minutes. (Right) Total number of inactive lever presses in 30 minutes. ns, non-significant and *P< 0.05 by unpaired t-test.
d. Breakpoint from the Progressive Ratio 3 (PR3) operant task for water in water deprived young and aged male and female mice. ns, non-significant and *P< 0.05 by unpaired t-test.
e. Schematic for stereotaxic injection of GRAB-DA dopamine sensor in the Nucleus Accumbens and implant of optic fiber for fiber photometry. NAc, Nucleus Accumbens. SFO, Subfornical Organ. VTA, Ventral Tegmental Area. Arrows represent synaptic projections.
f. GRAB-DA fiber photometry recording during water intake behavior after 24 hour water deprivation. (Top) Cumulative number of licks (blue) and mean z-score trace of GRAB-DA fluorescence in young (3-6 mo, black solid) and aged (24-26 mo, magenta solid) male and female mice, aligned by the first water lick bout (blue dotted vertical line). (Bottom) Heatmap of individual z-score traces in each group, aligned by the first water lick bout (black dotted vertical line).
g. Number of water licks during the first water lick bout in **f.** *P<0.05 by unpaired t-test.
h. Area under the curve of z-score of GRAB-DA fluorescence during 3 minutes after the first water lick bout after 24-hour water deprivation in **f.** **P<0.01 by unpaired t-test.
i. Schematic summary of our findings from neural recording.

bioRxiv preprint doi: https://doi.org/10.1101/2024.09.26.615271; this version posted September 27, 2024. The copyright holder for this preprint (which was not certified by peer review) is the author/funder, who has granted bioRxiv a license to display the preprint in perpetuity. It is made available under aCC-BY-NC-ND 4.0 International license.

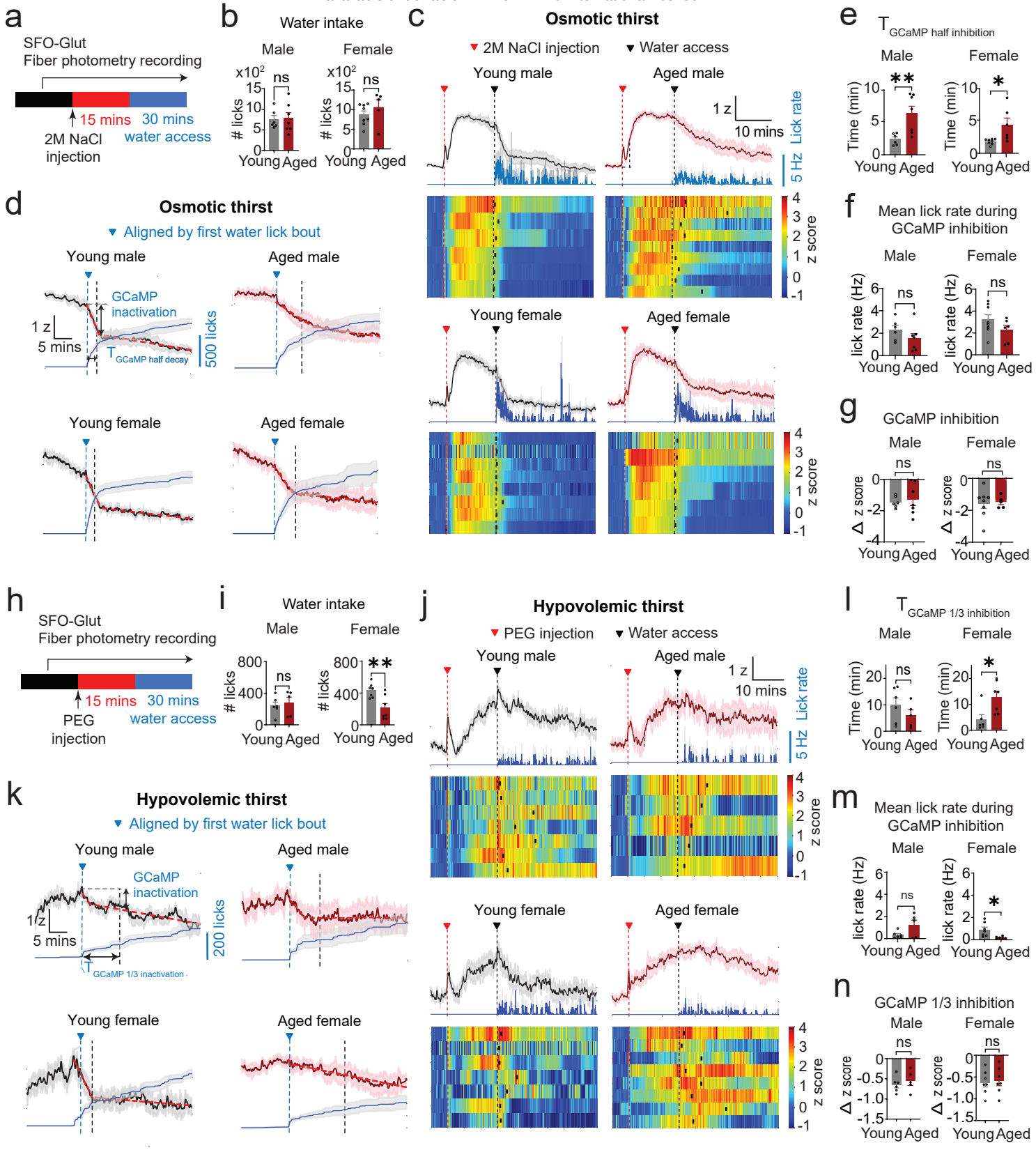

bioRxiv preprint doi: https://doi.org/10.1101/2024.09.26.615271; this version posted September 27, 2024. The copyright holder for this preprint (which was not certified by peer review) is the author/funder, who has granted bioRxiv a license to display the preprint in perpetuity. It is made available under aCC-BY-NC-ND 4.0 International license.

Figure 8. Age delays SFO^{Glut} neuronal inhibition by rehydration after osmotic and hypovolemic thirst.
a. Experimental paradigm for SFOGlut fiber photometry and behavioral recording for osmotic thirst induced by acute intraperitoneal 2 M NaCl injection.
b. Number of total water licks during 25 minutes. n.s., non-significant.
c. (Top) Mean lick rate (blue) and mean z-score trace of GCaMP fluorescence in young (4-7 mo, black solid) and aged (24-29 mo, magenta solid) male and female mice, aligned by 2 M NaCl injection (red dotted vertical line). (Bottom) Heatmap of individual z-score traces in each group. Black dotted lines represent water access. A black rectangle represents the beginning of water lick bout in each recording.
d. Cumulative number of water licks (gray solid) and mean z-score of GCaMP fluorescence in young male and female mice (black solid) in aged male and female mice (magenta solid), aligned by the first water lick bout (blue dotted vertical line with a blue triangle).
e. Time for GCaMP to decay from the peak to its half value of z-score as indicated in k (between t=0 in blue dotted vertical line and black dotted vertical line). *P<0.05 and **P<0.01 by unpaired t-test.
f. Mean lick rate during the fast SFO inhibition phase. n.s., non-significant by unpaired t-test.
g. Magnitude of SFO inhibition during the fast SFO inhibition phase as indicated in e. n.s., non-significant by unpaired t-test.
h. Experimental paradigm for SFO-Glut fiber photometry recording for hypovolemic thirst induced acute subcutaneous PEG injection.
i. Number of total water licks during 25 minutes. n.s., non-significant and **P<0.01 by unpaired t-test.